

# Integrated Bayesian Multi-model Approach to Quantify Input, Parameter and Conceptual Model Structure Uncertainty in Groundwater Modeling

Syed Md. Touhidul Mustafa <sup>1,\*</sup>, Jiri Nossent <sup>1,2</sup>, Gert Ghysels <sup>1</sup> and Marijke Huysmans <sup>1</sup>

<sup>1</sup>Department of Hydrology and Hydraulic Engineering, Vrije Universiteit Brussel (VUB), Brussels, Belgium

<sup>2</sup>Flanders Hydraulics Research, Department of Mobility and Public Works, Flemish Government, Antwerp, Belgium

**\* Correspondence:**

Syed Md. Touhidul Mustafa (e-mail: syed.mustafa@vub.be)

## 1 Highlights

- 2 • Full Bayesian multi-model approach to quantify uncertainty of MODFLOW model
- 3 • Simultaneously quantifies model structure, input and parameter uncertainty
- 4 • DREAM with a novel likelihood function is combined with BMA
- 5 • Neglecting conceptual model uncertainty results in unreliable prediction
- 6 • Results in more reliable model predictions and accurate uncertainty bounds

7

## 8 Abstract

9 A flexible Integrated Bayesian Multi-model Uncertainty Estimation Framework (IBMUEF) is  
10 presented to simultaneously quantify conceptual model structure, input and parameter  
11 uncertainty of a groundwater flow model. In this fully Bayesian framework, the DiffeRential  
12 Evolution Adaptive Metropolis (DREAM) algorithm with a novel likelihood function is  
13 combined with Bayesian Model Averaging (BMA). Four alternative conceptual models,  
14 representing different geological representations of an overexploited aquifer, have been  
15 developed. The uncertainty of the input of the model is represented by multipliers. A novel  
16 likelihood function based on a new heteroscedastic error model is included to extend the  
17 applicability of the framework. The results of the study confirm that neglecting conceptual

18 model structure uncertainty results in unreliable prediction. Consideration of both model  
19 structure and input uncertainty are important to obtain confident parameter sets and better  
20 model predictions. This study shows that the IBMUEF provides more reliable model  
21 predictions and accurate uncertainty bounds.

22 **Keywords: Conceptual model structure uncertainty, Bayesian approach, Input**  
23 **uncertainty, Bayesian model averaging, Uncertainty quantification, Groundwater flow**  
24 **model.**

## 25 **1. Introduction**

26 The reliability of predictions of numerical groundwater flow models is strongly influenced by  
27 different sources of uncertainty. To ensure reliable predictions and decision support in  
28 sustainable water resources management, it is important to assess all different sources of  
29 uncertainty. Conceptual model structure uncertainty can be related to the complexity of a  
30 groundwater model (Elshall and Tsai, 2014), which may vary from a simple to a detailed  
31 representation of the processes and geological information of the groundwater system (Rojas  
32 et al., 2010; Mustafa et al., 2019). The geological structure is often very complex and  
33 heterogeneous and only partially known. Hence, the incomplete and biased representation of  
34 the processes, and the complex structure of a system often result in uncertainty in model  
35 predictions (Refsgaard et al., 2006; Rojas et al., 2008).

36 It is important to assess the different sources of uncertainty to ensure accurate predictions and  
37 reliable decision support in sustainable water resources management. The conventional  
38 treatment of uncertainty in groundwater modeling primarily focuses on parameter  
39 uncertainty, whereas uncertainties due to the model structure are often neglected (Gaganis &  
40 Smith, 2006; Rojas et al., 2008). However, many researchers have recently acknowledged  
41 that the uncertainty arising from the conceptual model structure has a significant effect on the  
42 model predictions and that parameter uncertainty does not cover the whole range of  
43 uncertainty (Bredehoeft, 2005; Højberg & Refsgaard, 2005; Mustafa et al., 2018, 2019;  
44 Neuman, 2003; Poeter & Anderson, 2005; Refsgaard et al., 2006, 2007; Rojas et al., 2008;  
45 Trolborg et al., 2007). Therefore, neglecting conceptual model structure uncertainty may  
46 result in unreliable predictions and underestimation of the total predictive uncertainty.

47 Most of recent studies only consider a single conceptual model structure and may fail to  
48 adequately sample the relevant space of plausible conceptual models. Single model

49 techniques are unable to account for errors in model output resulting from structural  
50 deficiencies of a specific model as single models cannot capture all hydrogeological  
51 processes of the system (Ajami et al., 2007; Rojas et al., 2008; Mustafa et al., 2019). As a  
52 consequence, a well-calibrated model does not always accurately predict the behavior of the  
53 dynamic system (Van Straten & Keesman, 1991). Choosing a single model out of equally  
54 plausible alternative models may contribute to either type I (reject true model) or type II (fail  
55 to reject false model) model errors (Li & Tsai, 2009; Neuman, 2003).

56 Bredehoeft (2005) has presented different examples where the collection of new data and  
57 unforeseen elements challenged well-established conceptual models. Hence, researchers in  
58 hydrogeological science have suggested to use different alternative conceptual models for a  
59 single hydrogeological system (Højberg & Refsgaard, 2005; Mustafa et al., 2019; Nettasana  
60 et al., 2012; Refsgaard et al., 2006; Troldborg et al., 2007). Such multi-model approaches can  
61 be used to estimate a broader uncertainty band so that it is more likely to include the  
62 unknown true predicted value (Rojas et al., 2010). However, conceptual model structure  
63 uncertainty arising from the simplified representation of the hydro(geo)logic processes,  
64 geological stratification and boundary conditions, has received less attention (Refsgaard et  
65 al., 2006; Rojas et al., 2010).

66 A model averaging technique can be used to combine predictions of multiple models.  
67 Hydrologists have been using different model averaging techniques to obtain an average  
68 prediction and a reliable uncertainty band from a number of plausible conceptual models  
69 (Vrugt, 2016a). The predictions of multiple models are combined by using weights, which  
70 can be equal or can be determined through regression-based approaches (Yin and Tsai, 2018).  
71 Poeter & Anderson (2005) have proposed an approach in which weights are connected to  
72 model performance and the predictions of the conceptual models are combined using  
73 Akaike's weights (Akaike, 1974). However, in the multi-model predictions, this approach  
74 does not consistently include prior knowledge about parameters and conceptual models.  
75 Refsgaard et al. (2006) have proposed a method to incorporate prior knowledge of multiple  
76 model structures. In this approach, a set of conceptual models are calibrated separately and  
77 the consistency of these models was assessed using pedigree analysis. However, this method  
78 does not provide results in a quantitative way that can be used to analyse uncertainty in terms  
79 of probabilities.

80 On the other hand, the Bayesian Model Averaging (BMA) method (Draper, 1994; Hoeting et  
81 al., 1999) derives predictions from a set of alternative conceptual models to construct a  
82 predictive uncertainty distribution using probabilistic techniques. The weights in the BMA  
83 method are assessed based on the relative performance of each model to reproduce system  
84 behavior during the observation period. Recently, BMA has received attention of researchers  
85 in diverse fields because of its more reliable and accurate predictions than other existing  
86 model averaging methods (Li & Tsai, 2009; Rojas et al., 2008, 2010; Singh et al., 2010;  
87 Troldborg et al., 2010; Vrugt, 2016a; Ye et al., 2004, 2010).

88 An important challenge in implementing Bayesian Model Averaging is evaluating Bayesian  
89 model evidence (BME). There are different techniques to evaluate BME, such as analytical  
90 techniques, mathematical approximations, and numerical evaluation. The analytical solution  
91 is strongly depended on the assumptions. That is why exact and computationally efficient  
92 analytical solutions are rarely available (Schoniger et al., 2014). There are different methods  
93 of mathematical approximation, such as Laplace approximation, Kashyap Information  
94 criterion, Bayesian Information Criterion and Akaike Information Criterion. Those different  
95 mathematical information criterions may provide contradictory results in model ranking and  
96 posterior model weights (Poeter and Anderson, 2005; Singh et al., 2010; Ye et al., 2010;  
97 Schoniger et al. 2014). However, awareness about the contradictory results from different  
98 methods is very limited (Hoge et al., 2019). Although numerical methods are as prone to be  
99 biased than mathematical approximations, Schoniger et al. (2014) have concluded that bias-  
100 free numerical evaluation methods are better than mathematical approximations for model  
101 selection. Among the numerical evaluation methods, the multi-chain Markov Chain Monte  
102 Carlo (MCMC) based DiffeRential Evolution Adaptive Metropolis (DREAM) algorithm  
103 became very popular because of its statistical robustness and numerical efficiency (Leta et al.,  
104 2015; Vrugt et al., 2008, 2016; Laloy et al., 2013; ). However, applications of this algorithm  
105 for quantifying conceptual structural uncertainty of a real-world groundwater flow model also  
106 considering uncertainties from the model input and parameters are very limited.

107 Maximum Likelihood Bayesian Model Averaging (MLBMA), which is an approximation of  
108 BMA, has been applied recently in hydrogeology to analyse the predictive distribution of  
109 several conceptual models (Neuman, 2003; Ye et al., 2004). MLBMA depends on the  
110 calibration of alternative conceptual model parameters. However, by using this method  
111 estimated biased parameters will compensate conceptual model structure errors during  
112 calibration to obtain the best model fit (Højberg & Refsgaard, 2005; Refsgaard et al., 2006;

113 Trolborg et al., 2007). Refsgaard et al. (2006) have reported that the model becomes biased  
114 when calibrated models are used for simulating variables that were not included in  
115 calibration.

116 However, the existing Bayesian averaging approach does not quantify the uncertainty arising  
117 from the different components of the individual conceptual model and how they affect the  
118 model prediction (Tsai, 2010; Gupta et al., 2012; Tsai and Elshall, 2013). Tsai and Elshall  
119 (2013) and Chitsazan and Tsai (2015) address this issue by introducing the Hierarchical  
120 BMA (HBMA) method. In this HBMA method, the uncertainty arising from the different  
121 components of the individual conceptual model is considered using a BMA tree.

122 Alternative approaches to account for conceptual model structure uncertainty along with  
123 uncertainty from other sources are integrated uncertainty assessment approaches, which  
124 combine estimation of individual sources of uncertainty into an integrated modeling  
125 framework. In surface water hydrology, two distinct approaches have been developed and  
126 applied: Bayesian total error analysis (BATEA) (Kavetski et al., 2006a, 2006b; Kuczera et  
127 al., 2006) and the integrated Bayesian uncertainty estimator (IBUNE) (Ajami et al., 2007).  
128 Both methods consider model parameter, input and conceptual structural uncertainties to  
129 quantify model prediction uncertainties. However, model ranking or multi-model  
130 combinations are not considered in the BATEA framework. Hence, diagnostic model  
131 comparison is not possible in this framework. On the other hand, the IBUNE framework  
132 allows to combine multi-model predictions based on model weights obtained from a non-  
133 Bayesian optimization algorithm. As a consequence, a robust Bayesian derivation of posterior  
134 probabilities is missing. To quantify input uncertainties, the IBUNE framework uses a  
135 multiplier that is assumed to be independent and normally distributed with fixed mean and  
136 variance. Vrugt and Robinson (2007) have criticized this assumption as it is not a very  
137 appropriate way to quantify model input and conceptual structural uncertainties. Furthermore,  
138 identification of spatial and temporal variation of the input multipliers is not possible in this  
139 framework as it considers only a single multiplier. The latter might result in a biased  
140 estimation of input uncertainties and thereby result in biased predictive uncertainty. As  
141 groundwater model input data, such as recharge and abstraction rates, are usually estimated  
142 using indirect methods or specific models which are not accurate and can present errors both  
143 in space and time, the IBUNE approach is often not suitable for groundwater modeling.

144 In the field of groundwater hydrology, however, no systematic integrated framework has  
145 been proposed to date. Rojas et al. (2008) have applied BMA in combination with the  
146 generalized likelihood uncertainty estimation (GLUE) method (Beven, 1993; Beven &  
147 Binley, 1992) to quantify conceptual model structure uncertainty. A three-dimensional  
148 hypothetical setup with three alternative conceptualizations has been considered to  
149 demonstrate the method. However, some researchers have criticized GLUE because it is not a  
150 formal Bayesian method and may result in statistically incoherent and unreliable parameters  
151 and predictive distributions (Mantovan & Todini, 2006; Montanari, 2005; Stedinger et al.,  
152 2008). Therefore, the likelihood and threshold used for model selection and weighting in the  
153 approach of Rojas et al. (2008) has a lack of statistical basis and, as a consequence,  
154 conceptual model structure and parameters are not optimized in this method, which could  
155 result in overestimation of predictive uncertainty (Nettasana et al., 2012).

156 Recently, Xue & Zhang (2014) have applied multimodel ensemble Kalman filter (EnKF) in  
157 combination with the Bayesian model averaging framework to explicitly consider the model  
158 structural uncertainty. They advocated that the EnKF is computationally more efficient  
159 compared to other existing Bayesian methods. However, uncertainty arising from model  
160 input and measurement heteroscedasticity has not been explicitly considered in this  
161 framework. The performance of this multimodel EnKF framework has been tested using  
162 synthetic 2D conceptual groundwater model in idealized conditions without consideration of  
163 observational uncertainty or model bias, whereas the real-world models are often three-  
164 dimensional and more complex, and observations are not bias free (Hoge et al. 2019). Ridler  
165 et al. (2018) have also criticized this multimodel EnKF framework because of its limitation in  
166 application with bias observation. Hendricks Franssen et al. (2011) reported that the EnKF  
167 significantly outperformed with synthetic experimental data compare the real data.

168 Mustafa et al. (2018) presented a Bayesian approach to simultaneously quantify parameter  
169 and input uncertainty of a groundwater flow model. The performance of this approach has  
170 been evaluated using a single conceptual real-world groundwater flow model. Groundwater  
171 recharge and groundwater abstraction multipliers with a spatial and temporal character have  
172 been introduced in this study to quantify the uncertainty of the spatially distributed input data  
173 of the groundwater model along with parameter uncertainty. Nevertheless, the conceptual  
174 model structural uncertainty has not been considered in this study. As a result, the latter study  
175 is unable to account for the errors in the model output resulting from the structural  
176 deficiencies. Recently, Mustafa et al. (2019) presented a multi-model approach to quantify

177 groundwater-level prediction uncertainty considering alternative conceptual models. In the  
178 second study, the combined effect of conceptual model structure, the climate change and  
179 groundwater abstraction scenarios on future groundwater-level prediction uncertainty has  
180 been evaluated. However, alternative conceptual models of this study have been calibrated  
181 using a local optimization method and considering only model parameter. As a result, this  
182 approach is unable to account for the uncertainty arising from the model input and  
183 parameters. Estimated biased parameters will compensate conceptual model structural errors  
184 during calibration to obtain the best model fit, as it relies on a single optimum parameter set.  
185 Moreover, the approach is missing the statistical robustness because of its deterministic  
186 modelling approach.

187 Very recently, Hoge et al. (2019) highlight the difference between BMA and Bayesian  
188 combined model averaging (BCMA) following Minka (2002) and Monteith et al. (2011).  
189 According to Hoge et al. (2019), BCMA means the application of equations for BMA  
190 (section 2.3) to forecast combinations of individual conceptual models instead of the  
191 application of equations for BMA to the individual conceptual model alternatives. Hoge et al.  
192 (2019) concluded that the objective of the modelling should be the main driver in selecting  
193 model averaging approaches. They also suggested to use BCMA instead of BMA if the  
194 objective of the modelling is to increase the reliability of the model prediction. The Integrated  
195 Bayesian Uncertainty Estimator (IBUNE) that has been applied in surface water hydrology  
196 by Ajami et al. (2007) has been considered as a practical application of applying BMA in  
197 similar fashion of BCMA (Hoge et al. 2019). However, as mentioned earlier, Ajami et al.  
198 (2007) allows to combine multi-model predictions based on model weights obtained from a  
199 non-Bayesian optimization algorithm. As a consequence, a robust Bayesian derivation of  
200 posterior probabilities is missing.

201 Hence, more research on a systematic integrated fully Bayesian framework is needed to  
202 quantify the uncertainty arising from the conceptual model structure, inputs and parameters  
203 of groundwater flow models with consideration of the heteroscedasticity of the groundwater  
204 level error. Additionally, the application of such an integrated multimodel framework on  
205 real-world cases is necessary to better understand the impacts of different sources of  
206 uncertainty on real-world model calibration and prediction problems.

207 The general objective of this study is therefore the development and application of an  
208 **Integrated Bayesian Multi-model Uncertainty Estimation Framework (IBMUEF)** to quantify

209 input, parameter, measurement and conceptual model structure uncertainty of a fully  
210 distributed physically-based groundwater flow model to provide reliable predictions of  
211 groundwater system. In the proposed integrated fully Bayesian multi-model framework, the  
212 DiffeRential Evolution Adaptive Metropolis (DREAM) algorithm with a specific likelihood  
213 function is combined with the Bayesian Model Averaging (BMA) framework. In this new  
214 DREAM-BMA methodology, a likelihood function has been included based on the novel  
215 heteroscedastic error model for groundwater levels proposed by Mustafa et al. (2018). Like  
216 IBUNE of Ajami et al. (2007), the current study uses equations for BMA in a similar fashion  
217 as BCMA. However, unlike Ajami et al. (2007), our study allows to combine multi-model  
218 predictions based on model weights obtained from a Bayesian optimization algorithm. This is  
219 the first attempt to apply a fully Bayesian multi-model framework in real-world groundwater  
220 modeling to quantify conceptual model structure uncertainty along with uncertainties  
221 originating from model input, parameters and measurement error. In this methodology, the  
222 fully Bayesian approach proposed by Mustafa et al. (2018) has been combined with the  
223 Bayesian Combined Model Averaging (BCMA) to simultaneously quantify the uncertainty  
224 arising from the conceptual model structural, input and parameter of a fully distributed  
225 groundwater flow model. Additionally, the proposed approach is applicable for all types of  
226 residual errors i. e. both for homoscedastic and heteroscedastic errors. The IBMUEF is a  
227 flexible framework as (i) there is no limitation for the number or complexity of alternative  
228 conceptual models, (ii) users can choose the number and dimensions (spatial and temporal) of  
229 input multipliers, (iii) both quantitative and qualitative information of the system can be used  
230 in the alternative conceptual models, and (iv) it is applicable for both homoscedastic and  
231 heteroscedastic residuals errors. Moreover, the proposed approach is able to avoid  
232 compensation for conceptual model structural uncertainty arising from biased parameter  
233 estimates obtained from a model fit, as it does not rely on a single optimum parameter set.

234 Finally, the framework (IBMUEF) is applied in an over-exploited aquifer in the north-  
235 western Bangladesh, as it is necessary to understand the impacts of conceptual model  
236 structural uncertainties on model prediction in realistic conditions. The specific objectives of  
237 this paper are: (i) to quantify model uncertainty originating from errors in model  
238 conceptualization, (ii) to quantify individual uncertainty contributions arising from model  
239 input, parameter, and measurement and conceptual model uncertainties, (iii) to understand  
240 conceptual model structure uncertainty impacts on calibration and model prediction, (iv) to



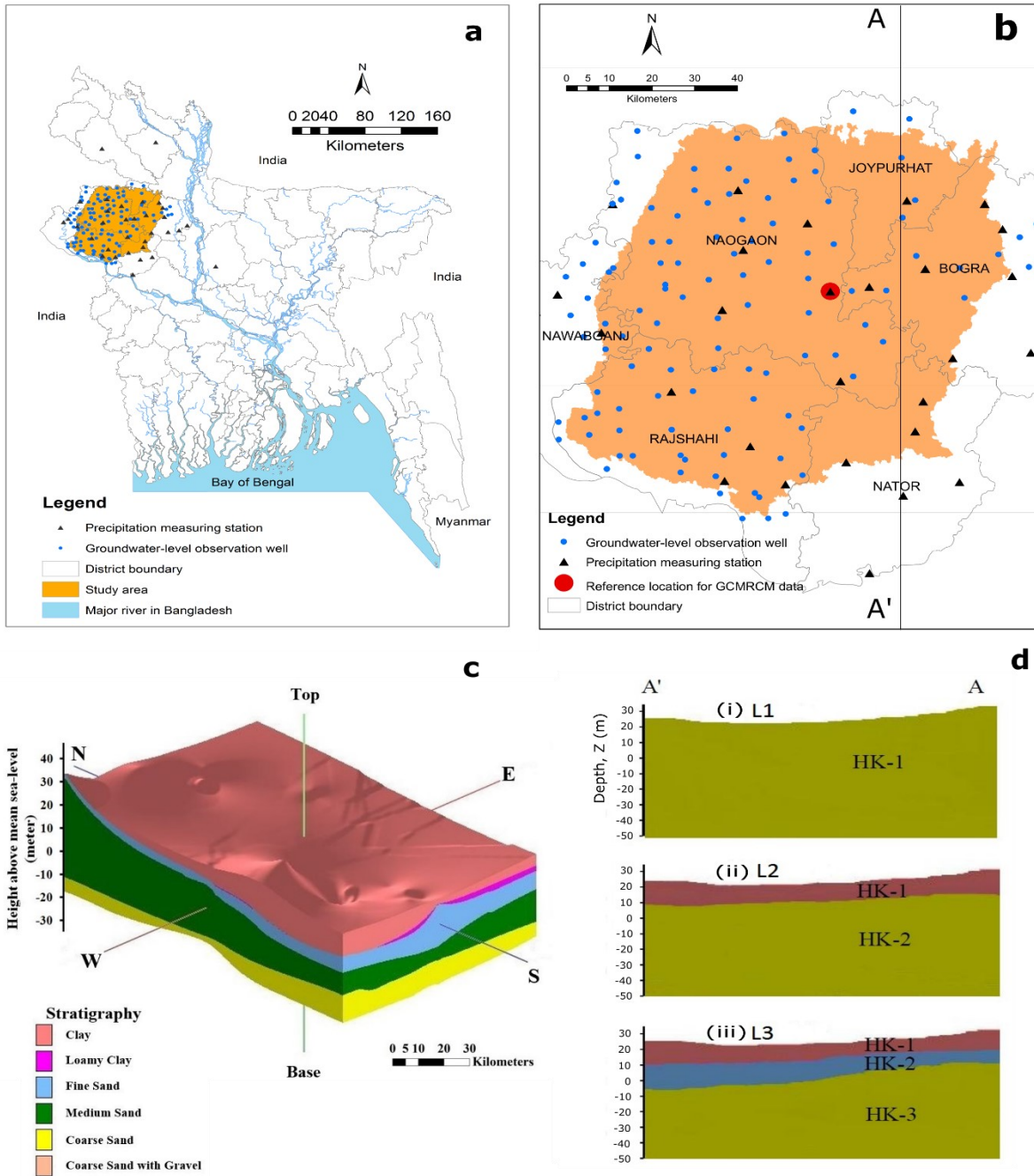
241 evaluate the applicability of our approach for groundwater models in realistic conditions  
242 using alternative conceptual groundwater flow models.

## 243 **2. Methodology**

### 244 **2.1 Study area**

245 The study area covers the six north-western districts of Bangladesh (Figure 1a). The aquifer  
246 consists mainly of medium sand, coarse sand and coarse sand with gravel, with minor  
247 fractions of clay, loamy clay, and fine sand (Figure 1c). The thickness of each stratigraphic  
248 unit moreover varies spatially. The average thickness of the top layer is 18 m and it consists  
249 of clay, clayey loam and fine sand. A 20 m thick medium sand layer is present below the top  
250 layer. The bottom part of the aquifer consists of a 35 m thick layer of coarse sand and coarse  
251 sand with gravel. Average rainfall is between 1400 mm and 1550 mm per year. However,  
252 rainfall distribution is not uniform over the year. There is almost no rainfall during the dry  
253 season (November to April), which is the major cropping season in this study area (Mustafa  
254 et al., 2017b). The area is mainly covered by irrigated agriculture of which more than 80 % is  
255 rice. Irrigated agriculture uses around 97 % of total groundwater abstraction (Shahid, 2009;  
256 Mustafa et al. 2017a). Groundwater level in this study area is continuously decreasing due to  
257 overexploitation of groundwater for irrigation (Mustafa et al., 2017a).

258



259

260 Figure 1: Description of the study area: (a) Location of the study area in the north-western  
 261 part of Bangladesh; (b) study area with precipitation measurement stations (triangles) and  
 262 groundwater observation wells (circles); (c) stratigraphy of the study area; (d) cross-sectional  
 263 (A-A') view of different hydrogeological models: (i) one-layered model (L1), (ii) two-layered  
 264 model (L2), (iii) three-layered model (L3). Taken from Mustafa et al. (2019).

265

## 266 2.2 Bayesian approach to quantify input and parameter uncertainty

267 Mustafa et al. (2018) presented a Bayesian approach to simultaneously quantify parameter  
268 and input uncertainty of a fully distributed groundwater flow model. For the details of the  
269 approach we refer the reader to Mustafa et al. (2018). A short summary of the approach is  
270 presented here. A hydrogeological model can be defined as follows:

$$O = M(\bar{I}, \theta, \eta) \quad (1)$$

271 Where  $\bar{I}$  and O represent the input and output matrix of model M;  $\theta$  and  $\eta$  are the parameters  
272 and boundary conditions of the corresponding model. To quantify input uncertainty along  
273 with parameter uncertainty, following Kavetski et al. (2002, 2006a, 2006b) a modified  
274 concept of multipliers for a fully distributed groundwater model has been introduced by  
275 Mustafa et al. (2018). The uncertainty of the input data (groundwater abstraction and  
276 recharge) is quantified using the following input error model:

$$I_{ij} = \bar{I}_{ij} * m_{ij} \quad (2)$$

277 Where  $\bar{I}_{ij} = \{\bar{I}_{1,1}, \bar{I}_{1,2}, \bar{I}_{1,3}, \dots, \dots, \bar{I}_{j,N}\}$  represents the initial input for the  $i^{\text{th}}$  month and  $j^{\text{th}}$   
278 location,  $m_{ij}$  is the respective input multiplier and  $I_{ij}$  represents the corresponding corrected  
279 input.  $m_R$  represents the groundwater recharge multipliers while  $m_A$  represents groundwater  
280 abstraction multipliers (Table 1). The multipliers are considered as an additional individual  
281 latent parameter and are estimated along with the model parameters.

282 Traditionally, residual errors in groundwater modelling are considered to be homoscedastic.  
283 However, Mustafa et al. (2018) have shown that the standard deviation of the groundwater  
284 level residual is not always constant but may increase with the deviation of groundwater level  
285 from the normal. In this study, the long-term average is considered as the normal  
286 groundwater level. A novel heteroscedastic error model for groundwater level has been  
287 proposed in this fully Bayesian approach to consider the heteroscedasticity of the  
288 groundwater level residual. The proposed heteroscedastic error model is defined as follows:

$$\sigma = A * |SH_i - \overline{OH}| + B \quad (3)$$

289

290 Where  $\sigma$  is standard deviation, A is a parameter representing the groundwater level  
291 uncertainty slope, B is a parameter representing the groundwater level uncertainty intercept,  
292  $SH_i$  represents the simulated groundwater level for each time step and  $\overline{OH}$  represents the  
293 observed long-term (30 years for this study) average groundwater level.

294 The log-likelihood function proposed by Vrugt et al. (2009a, 2013) has been adopted and  
 295 modified by Mustafa et al. (2018) for spatially distributed groundwater models. The proposed  
 296 novel heteroscedastic error model for groundwater level has been incorporated in this  
 297 modified log-likelihood function. The new log-likelihood function is as follows:

$$\ell(\theta|\bar{I}, \bar{O}, \eta) = -\frac{T}{2} \ln(2\pi) - \sum_{l=1}^L \left( \sum_{t=1}^T \ln(\sigma_{tl}) \right) - \frac{1}{2} \sum_{l=1}^L \left( \sum_{t=1}^T \left( \frac{\bar{O}_{tl} - O_{tl}}{\sigma_{tl}} \right)^2 \right) \quad (4)$$

298 Where  $\bar{O} = \{\bar{o}_1, \bar{o}_2, \bar{o}_3, \dots, \dots, \bar{o}_T\}$  represents the output series of observed groundwater  
 299 levels in observation wells,  $O = \{o_1, o_2, o_3, \dots, \dots, o_T\}$  represents the output series of  
 300 simulated groundwater levels for the same observation well,  $t = \{1, 2, 3, \dots, \dots, T\}$   
 301 represents time step, T represents the total number of time steps,  $l = \{1, 2, 3, \dots, \dots, L\}$   
 302 represents the location of the observation wells and L represents the total number of  
 303 observation wells.

304 This log-likelihood function has been used in this study because of (i) its numerical stability,  
 305 (ii) algebraic simplicity and (iii) its applicability for both homoscedastic and heteroscedastic  
 306 residual errors. To sample the posterior distribution based on the likelihood function  
 307 (Equation 4), the DREAM-ZS sampler has been used. The Differential Evolution Adaptive  
 308 Metropolis algorithm (DREAM) is a multi-chain Markov Chain Monte Carlo (MCMC)  
 309 simulation algorithm introduced by Vrugt et al. (2008; 2009a; 2009b). The DREAM-ZS  
 310 algorithm (Vrugt, 2016) has been used in this study to explicitly quantify the uncertainty  
 311 arising from model input and parameters of a groundwater flow model. More details about  
 312 the DREAM algorithm are explained in Vrugt et al. (2008; 2009a; 2009b) and Vrugt (2016).

313 In this study, we extend this approach to include conceptual model structure uncertainties and  
 314 we improve the methodology by combining it with Bayesian Model Averaging (BMA).

### 315 **2.3 Bayesian Model Averaging (BMA)**

316 Bayesian Model Averaging is a probabilistic scheme for combining predictions from multiple  
 317 conceptual models to provide a more realistic and reliable description of total prediction  
 318 uncertainty. It is a technique that can be used to account for model structural uncertainty  
 319 (Madigan et al., 1996). It is a statistical procedure that derives average predictions by  
 320 weighing predictions from different models in such a way that the weighted prediction is a  
 321 better representation of the observed system variables compared to any individual model of  
 322 the ensemble. The BMA prediction gives higher weights to better performing models, as the

323 agreement between the model predictions and the observations is assumed to be a measure of  
 324 the model likelihood. The variance of BMA is a measure of the uncertainty of BMA  
 325 prediction. The variance of BMA predictions is representing both the within-model variance  
 326 and the between-model variance.

327 Bayesian Model Averaging (BMA) has been used to deduce more reliable predictions of  
 328 groundwater levels than the predictions produced by the different individual groundwater  
 329 models. Draper (1994) and Hoeting et al. (1999) present an extensive overview of BMA.  
 330 Here, only a short summary of BMA is given.

331 Consider  $\mathbf{M} = [M_1, M_2, M_3, \dots, M_K]$  the set of alternative conceptual models,  $\mathbf{Y} =$   
 332  $\{y_1, y_2, \dots, y_n\}$  is a  $1 \times n$  observation vector of a quantity of interest,  $F_{jk}$  is the point forecast  
 333 of each alternative conceptual model for  $j = \{1, 2, \dots, n\}$  observations and  $k = \{1, 2, \dots, K\}$   
 334 models. Now by combining the different conceptual models forecasts in a matrix  $\mathbf{F}$  having  
 335 dimensions of  $n \times K$ , the weighted average forecast of the quantity of interest is

$$y_j = \sum_{k=1}^K \beta_k F_{jk} + e_j \quad (5)$$

336 Where  $\beta = \{\beta_1, \beta_2, \dots, \beta_K\}$  represents the weight vector of each conceptual model and  $e_j$  is  
 337 noise.

338 As we know, model predictions are associated with uncertainty. The uncertainty can be  
 339 described using a probability density function (forecast distribution)  $p(\cdot)$ . When applying  
 340 BMA, assuming uniform prior distribution the posterior predictive distribution of the quantity  
 341 of interest is given by

$$p(y_j | F_{jk}) = \sum_{k=1}^K p(y_j | F_{jk}, M_k) p(M_k | F_{jk}) \quad (6)$$

342 Where,  $p(\cdot | \cdot)$  = conditional probability density function (PDF),  $p(y_j | F_{jk}, M_k)$  = posterior  
 343 predictive distribution of  $y_j$  on  $F_{jk}$  under the considered model  $M_k$  and  $p(M_k | F_{jk}) =$   
 344 posterior probability of the respective model  $M_k$ . This is also known as the likelihood  
 345 (weight) of the corrected model  $M_k$ .

346 The BMA predictive mean and variance of  $y$  are conditional to the discrete ensemble of the  
 347 proposed alternative conceptual models,  $\mathbf{M}$  (Draper, 1994).

$$E[y_j|F_{jk}] = E_{\mathbf{M}}[E(y_j|F_{jk}, \mathbf{M})] = \sum_{k=1}^K E[y_j|F_{jk}, M_k] p(M_k|F_{jk}) \quad (7)$$

348

$$\begin{aligned} Var[y_j|F_{jk}] &= E_{\mathbf{M}}[Var(y_j|F_{jk}, \mathbf{M})] + Var_{\mathbf{M}}[E(y_j|F_{jk}, \mathbf{M})] \\ &= \sum_{k=1}^K Var[y_j|F_{jk}, M_k] p(M_k|F_{jk}) + \sum_{k=1}^K (E[y_j|F_{jk}, M_k] - E[y_j|F_{jk}])^2 p(M_k|F_{jk}) \end{aligned} \quad (8)$$

349

350 Where  $E[y_j|F_{jk}, M_k]$  and  $Var[y_j|F_{jk}, M_k]$  represent , respectively, the expected value and  
 351 variance of  $y_j$  on  $F_{jk}$  under the considered conceptual model,  $M_k$ . Considering  
 352  $E[y_j|F_{jk}, M_k] = y_k$  ,  $Var[y_j|F_{jk}, M_k] = \sigma_k^2$  and  $p(M_k|F_{jk}) = \beta_k$ , the BMA predictive mean  
 353 and variance of the quantity of interest can be developed as follows

$$E[y_j|F_{jk}] = \sum_{k=1}^K y_k \beta_k \quad (9)$$

354

$$Var[y_j|F_{jk}] = \sum_{k=1}^K \sigma_k^2 \beta_k + \sum_{k=1}^K \beta_k \left( y_k - \sum_{u=1}^K y_u \beta_u \right)^2 \quad (10)$$

355 The first term of the variance is representing the within-model variance, while the second  
 356 term represents the between-model variance.

357 The BMA method considers the uncertainty of each model's forecast and uses it to develop a  
 358 predictive distribution rather than only a weighted average. So, the BMA method provides an  
 359 average forecast along with an associated forecast distribution. The forecast distribution can  
 360 be used for constructing confidence intervals. This BMA forecast density enforces one  
 361 significant constraint for the weights, i.e.,  $\beta_k \geq 0$  and  $\sum_{k=1}^K \beta_k = 1$  to avoid the development of  
 362 unrealistic forecast distributions (e.g., densities can even become negative without this  
 363 restriction). For successful application of the BMA method, proper estimates of the weights,  
 364 and standard deviation, of the normal conditional pdfs of the ensemble members are needed.  
 365 To estimate the weights and standard deviation, the log-likelihood function is used for  
 366 algebraic simplicity and numerical stability,

$$\mathcal{L}(\beta_{BMA}, \sigma_{BMA} | \mathbf{F}, \mathbf{Y}) = \sum_{j=1}^n \log \left\{ \sum_{k=1}^K \beta_k \frac{1}{\sqrt{2\pi\sigma_k^2}} \exp \left[ -\frac{1}{2} \sigma_k^{-2} (y_j - F_{jk})^2 \right] \right\} \quad (11)$$

367 where  $\beta_{BMA}$  is maximum likelihood Bayesian weight.

368 Equation (11) can only be solved iteratively. In this study, Markov Chain Monte Carlo  
 369 (MCMC) simulations based on the Differential Evolution Adaptive Metropolis (DREAM)  
 370 algorithm are used to calculate the log-likelihood function. The value of  $\beta_{BMA}$  was used as a  
 371 criterion to select better performing models that have a significant contribution in model  
 372 averaging.

### 373 **2.4 Integrated Bayesian Multi-model Uncertainty Estimation Framework (IBMUEF)**

374 In this framework, the fully Bayesian approach using input uncertainty multipliers based on a  
 375 specific heteroscedastic error-model as explained in section 2.2 is combined with the  
 376 Bayesian Model Averaging (BMA) framework explained in section 2.3. The IBMUEF  
 377 framework is implemented as follows:

- 378 1. A number of alternative conceptual hydrogeological models are proposed based on  
 379 the existing geological and hydrogeological information about the study area.
- 380 2. Along with parameter uncertainty, the input uncertainty of the spatially distributed  
 381 input data are quantified by using groundwater recharge and groundwater abstraction  
 382 multipliers (Section 2.2 and Mustafa et al., 2018).
- 383 3. A heteroscedastic error model is defined to quantify the heteroscedasticity of the  
 384 groundwater level residual (Section 2.2).
- 385 4. Hydrologically reasonable prior ranges are defined for the model parameters, input  
 386 multipliers and heteroscedastic error model parameters of each model (assuming a  
 387 uniform prior distribution).
- 388 5. A likelihood function is defined. The likelihood function is explained in section 2.2  
 389 and Mustafa et al. (2018).
- 390 6. The posterior distributions of model parameters, input multipliers and the  
 391 heteroscedastic error model parameters are obtained for each model after convergence  
 392 using DREAM.
- 393 7. A pre-specified number of outputs (e.g., groundwater levels) are generated for each  
 394 model, using the parameter values obtained from steps 2–6.

- 395 8. The model weights and variances of each ensemble member are calculated using the  
396 DREAM algorithm as explained in section 2.3.
- 397 9. The model weights are computed by summing the weights for all selected ensemble  
398 members of each conceptual model.
- 399 10. Finally, multi-model predictions are obtained by assessing predictive mean and  
400 variance using equations 7 and 8.

## 401 **2.5 Alternative conceptual models**

402 Hoge et al. (2019) concluded in their review paper that selection of alternative conceptual  
403 models is the most important aspect of Bayesian Model Averaging. Enemark et al. (2019)  
404 present a review of the conceptual hydrogeological model development. In our study, four  
405 alternative conceptual groundwater flow models have been selected from 15 possible  
406 alternative conceptual groundwater flow models. These initial 15 conceptual groundwater  
407 flow models were constructed using different geological interpretations and boundary  
408 conditions.

409 All alternative conceptual models were calibrated using observed groundwater level data for  
410 the same period. The performance of each model was evaluated based on different  
411 performance evaluation coefficients and information criterion statistics. Details about model  
412 development, calibration, evaluation and selection are provided in Mustafa et al. (2019).  
413 Obviously, the best option would be to use all 15 conceptual models. However, it would be  
414 computationally very expensive. Nevertheless, our main objective is not to predict the  
415 groundwater level of this study area. Rather our objectives are (i) to develop an integrated  
416 uncertainty quantification methodology that can quantify different sources of uncertainty of a  
417 groundwater flow model and thereby increase the reliability of the model prediction and (ii)  
418 the demonstration of the applicability of the proposed approach with real-world mode using  
419 simple personal computer. Therefore, the four best performing conceptual models were  
420 selected to reduce the computational effort in the Bayesian methodology. However, spatial  
421 heterogeneity of the aquifer properties is not considered as a part of conceptual model  
422 uncertainty. Peeters and Turnadge (2019) recommended based on their hypothetical setup  
423 that, for an aquifer with high recharge and high conductivity, spatial heterogeneity of the  
424 aquifer properties should be considered in developing a groundwater flow model. Hence,  
425 further studies could be conducted considering other alternative conceptualizations including  
426 spatial heterogeneity of the aquifer properties.



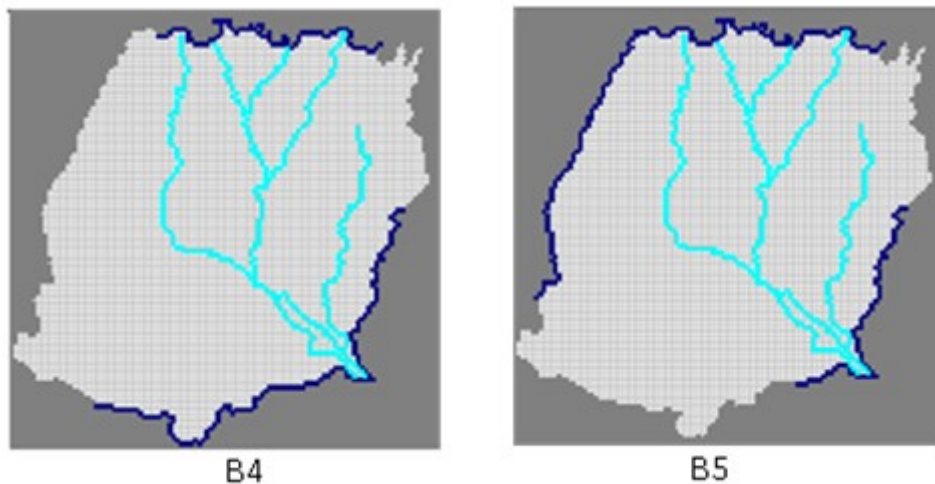
427 Later, the IBMUEF methodology has been implemented using the better performing four  
428 alternative conceptual models. The four selected alternative groundwater models are: (i) a  
429 one-layer model with boundary condition-5 (L1B5), (ii) a two-layer model with boundary  
430 condition-5 (L2B5), (iii) a two-layer models with boundary condition-4 (L2B4) and (iv) a  
431 three-layer models with boundary condition-5 (L3B5). Details about the selected conceptual  
432 models and model setup are explained in section 2.5.1 and 2.5.2.

### 433 **2.5.1 Alternative conceptual models development**

434 A cross sectional (A-A') view of the simplified hydrogeological models is shown in Figure  
435 1d. First, three simplified alternative conceptual groundwater models were defined based on  
436 the geological stratification. The three models are a one-layered (L1), a two-layered (L2) and  
437 a three-layered (L3) model setup as shown in figure 1d. The bottom elevation of the aquifer  
438 in model was taken 50 m below sea level. In the one-layered model (L1), the whole model  
439 domain was considered as one hydro-stratigraphic unit and it was assumed that hydraulic  
440 properties are homogeneous and isotropic. The two-layered model (L2) consists of two layers  
441 where the average thickness of the top layer was 10 m (clay and loamy clay soil) and rest of  
442 the thickness was considered as the bottom layer. The model domain was divided into three  
443 different hydro-stratigraphic units to develop a three-layered model (L3). The top layer of the  
444 three-layered model was the same as for the two-layered model, but just below the top layer,  
445 a fine sand layer with an average thickness of 8 m was added in the three-layered model. The  
446 bottom layer of three-layered model consists of medium sand, coarse sand and coarse sand  
447 with gravel. Four or more layered models were not considered in this study because the  
448 information of the exact positions of the groundwater abstraction wells filter was unknown.  
449 Therefore, a further increase in layer numbers would increase the complexities of placing  
450 groundwater abstraction wells in the model domain.

451 One of the major factors that influences conceptual model uncertainty is related to the  
452 boundary conditions of the model (Wu & Zeng, 2013). Boundary conditions of groundwater  
453 models are often very uncertain, although the model results largely depend on these boundary  
454 conditions. A previous study in the Bengal basin observed that groundwater flows from north  
455 to south (Michael & Voss, 2009a, 2009b). On the other hand, there is a large wetland at the  
456 southeastern corner of the study area, as well as a large river (known as Ganges/Padma)  
457 within a few kilometers from the south boundary. Since exact boundary conditions were not  
458 known, five different potential sets of boundary conditions were conceptualized based on the

459 above information. In this study, two sets of boundary conditions are used after an initial  
460 evaluation (Figure 2). Detailed description of the other boundary conditions and the  
461 evaluation procedure are explained in Mustafa et al. (2019). In boundary condition 4 (B4), a  
462 constant head boundary was considered on the north side of the model, where most of the  
463 river branches originate, assuming that groundwater flow direction is parallel to the river  
464 flow, and the southeastern part of the model, where a large wetland is located. At the south  
465 part of the model domain, a constant head is assigned because the great Ganges/Padma river  
466 is very near to the south boundary. In boundary condition 5 (B5), at the north and north-  
467 western boundary also at the south-eastern corner of the model domain, a constant head  
468 boundary was considered, based on the information that groundwater is flowing from north  
469 and northwestern to south in the study area (Michael & Voss, 2009a, 2009b). A constant head  
470 is assigned at the south-eastern corner of the model domain to represent the Chalan Beel  
471 wetland. The south and north-eastern boundaries are parallel to groundwater flow direction  
472 (Michael & Voss, 2009a, 2009b) hence no-flow boundaries are assigned at the south and  
473 north-eastern boundaries.



474

475 Figure 2: Alternative boundary conditions used to develop alternative conceptual model (blue  
476 line indicates constant head boundary): B4: constant head at north, south and southeast  
477 boundary; B5: constant head at north, northwestern and southeastern boundary.

### 478 2.5.2 Model setup and data

479 PMWIN: Processing MODFLOW (Chiang & Kinzelbach, 1998) is a grid based, fully-  
480 distributed, physically-based, integrated simulation system for modelling groundwater flow  
481 and solute transport processes and was used for groundwater flow simulations. The study area

482 having an area of 7112 km<sup>2</sup> was discretized into smaller cells, resulting in 117 rows and 118  
483 columns of grid cells, with a dimension of 900 m x 900 m. All the alternative conceptual  
484 models are transient with a monthly time step. A no-flow boundary is considered at the model  
485 domain bottom as vertical groundwater flow is restricted by the relatively impermeable hard  
486 rock below the aquifer in the study area. On the model top surface, a spatially distributed  
487 recharge boundary is considered. Spatially distributed monthly groundwater recharge was  
488 simulated using the WetSpas-M model with the same grid cell size as the MODFLOW  
489 model (Abdollahi et al., 2017; Batelaan & De Smedt, 2007). The study area was divided into  
490 34 abstraction zone considering each upazila as one zone (upazila is the second lowest tier of  
491 regional administration in Bangladesh). Groundwater abstraction in each zone was calculated  
492 using an empirical relation based on the irrigated area and crop irrigation requirements.  
493 Details about the estimation of the groundwater abstraction and simulation of groundwater  
494 recharge can be found in Mustafa et al. (2017a).

495 The initial groundwater heads correspond to a long-term average groundwater table obtained  
496 by running the models in steady state conditions.

497 Weekly groundwater level and daily rainfall data were collected from the Water Resources  
498 Planning Organization (WARPO), Bangladesh. The groundwater level and rainfall were  
499 collected respectively for 140 and 30 sites. Available river discharge data of the BWDB for  
500 the existing small rivers within the study area were also collected from WARPO. Daily  
501 maximum and minimum temperature, wind speed and other climatic data were collected from  
502 the Bangladesh Meteorological Department (BMD). Reference evapotranspiration ( $ET_0$ ) was  
503 calculated using the FAO Penman-Monteith equation (Allen et al., 1998; Mustafa et al.,  
504 2017a,b). In this study, reference evapotranspiration ( $ET_0$ ) is also considered as potential  
505 evapotranspiration.

506 The monthly observed groundwater level data of 50 observation wells have been used for  
507 model calibration and validation (Figure 1b).

508 Topography and borehole data were collected from Bangladesh Multipurpose Development  
509 Authority (BMDA). The geological and lithological log data from twenty-three boreholes  
510 within the study area were collected from BMDA.

## 511 **2.6 Parameterization**

512 Groundwater recharge multipliers and groundwater abstraction multipliers have been  
513 introduced to quantify uncertainty of the estimated spatially distributed groundwater recharge

514 and abstraction data. The input multipliers are considered as additional individual latent  
 515 parameters during model calibration and uncertainty analysis and have been estimated along  
 516 with model parameters. The hydrologically acceptable ranges of the multipliers have been  
 517 defined based on the available knowledge of the possible level of bias in the initial estimation  
 518 of groundwater recharge and abstraction (Table 1). In addition to the input multipliers, the  
 519 following influential MODFLOW parameters have been considered: (i) Horizontal hydraulic  
 520 conductivity, (ii) Specific yield, (iii) Hydraulic conductance of Riverbed and (iv) Specific  
 521 storage. The first three MODFLOW parameters have been considered for the one-layered  
 522 model. For the two- and three-layered models, specific storage has also been added.  
 523 Considering specific parameters for each layer results in, respectively, seven and ten  
 524 MODFLOW parameters to be considered for the two- and three-layered models (Table 1).  
 525 The selected parameters and their prior uncertainty ranges are presented in Table 1.

526 A uniform prior probability distribution within the hydrologically acceptable ranges has been  
 527 considered as a prior range for each parameter (Table 1) as we have no information about the  
 528 distribution of the prior. Moreover, this is the most widely used prior in case of limited  
 529 information availability about the distribution of the parameter value (Enemark et al. 2019).  
 530 The range of hydrogeological parameter values was selected based on typical values for  
 531 aquifer materials (Domenico & Mifflin, 1965; Domenico & Schwartz, 1998; Johnson, 1967)  
 532 and previous research findings in the study area (Michael & Voss, 2009a, 2009b). Although  
 533 the number of MODFLOW parameters is different for different conceptual model structures,  
 534 the input multipliers and heteroscedastic error model parameters remain the same for all  
 535 conceptual models (Table 1).

536 Table 1: Parameters of the alternative conceptual models, input multipliers and  
 537 heteroscedastic error model parameters used in the uncertainty analysis using IBMUEF with  
 538 their prior ranges

	<b>Descriptions</b>	<b>Unit</b>	<b>Ranges</b>
<b>Input parameters for all models</b>			
$m_R$	Groundwater recharge multipliers	-	0.010 – 10
$m_A$	Groundwater abstraction multipliers for temporal changes	-	0.010 – 10
<b>The parameters of the heteroscedastic error model to consider heteroscedasticity of the groundwater level error</b>			

A	Groundwater level uncertainty slope	-	0.010 – 1.0
B	Groundwater level uncertainty intercept	m	0.010 – 3.0
<b>Model parameters of one-layer models (L1B5)</b>			
HK	Horizontal hydraulic conductivity	m/s	0.0000001 – 0.0095
RIVC	Hydraulic conductance of Riverbed	m <sup>2</sup> /s	0.001 – 1.6
SY	Specific yield	-	0.10 – 0.35
<b>Model parameters of two-layer models (L2B5, L2B4)</b>			
HK-1	Horizontal hydraulic conductivity of layer-1	m/s	0.0000001 – 0.0095
HK-2	Horizontal hydraulic conductivity of layer-2	m/s	0.0000001 – 0.0095
RIVC	Hydraulic conductance of Riverbed	m <sup>2</sup> /s	0.001 – 1.6
SY-1	Specific yield of layer-1	-	0.10 – 0.35
SY-2	Specific yield of layer-2	-	0.10 – 0.35
SS-1	Specific storage multipliers of layer-1	-	0.015 – 15
SS-2	Specific storage multipliers of layer-2	-	0.015 – 15
<b>Model parameters of three-layer models (L3B5)</b>			
HK-1	Horizontal hydraulic conductivity of layer-1	m/s	0.0000001 – 0.0095
HK-2	Horizontal hydraulic conductivity of layer-2	m/s	0.0000001 – 0.0095
HK-3	Horizontal hydraulic conductivity of layer-3	m/s	0.0000001 – 0.0095
RIVC	Hydraulic conductance of Riverbed	m <sup>2</sup> /s	0.001 – 1.6
SY-1	Specific yield of layer-1	-	0.10 – 0.35
SY-2	Specific yield of layer-2	-	0.10 – 0.35
SY-3	Specific yield of layer-3	-	0.10 – 0.35
SS-1	Specific storage multipliers of layer-1	-	0.015 – 15
SS-2	Specific storage multipliers of layer-2	-	0.015 – 15
SS-3	Specific storage multipliers of layer-3	-	0.015 – 15

539

## 540 2.7 Computational experiments

541 Three different scenarios have been used to perform uncertainty analysis along with model  
542 calibration. The model parameters and heteroscedasticity of groundwater level error have  
543 been considered in the first scenario. In this scenario, the input data are considered perfectly  
544 known and accurate. This scenario will serve as a benchmark. In the second scenario, model  
545 parameters, heteroscedasticity of the groundwater level error and temporal groundwater

546 abstraction and recharge multipliers are considered. In this scenario, we introduced 12  
547 groundwater recharge multipliers ( $m_R$ ) to describe uncertainties in groundwater recharge,  
548 assigning a single multiplier corresponding to each time step which is one month in this  
549 study. Similarly, we introduced 6 groundwater abstraction multipliers ( $m_A$ ) to describe  
550 uncertainties in groundwater abstraction, assigning a single multiplier corresponding to each  
551 time step. Abstraction multipliers have been considered only for the dry season (November to  
552 April), because this is the major abstraction period for irrigation in the study area. Details on  
553 estimation and uncertainty analysis of groundwater recharge and abstraction can be found in  
554 Mustafa et al. (2018).

555 Abstraction multipliers associated with the spatial estimation have been excluded in this  
556 study because of computational time although they might have considerable effect on the  
557 model prediction. In this study, four alternative conceptual groundwater models have been  
558 used with different levels of complexity. The computational time increases with increased  
559 complexity of the alternative conceptual groundwater models. For example, for the three-  
560 layer model with a total of 64 parameters (including both spatial and temporal abstraction  
561 multipliers), the algorithm has not reached convergence even after 200000 model evaluations.  
562 On a 2.70 GHz processor, 200000 model evaluations take around 21 days with an average of  
563 9 seconds per simulation. Similarly, for the two-layered model with a total of 61 parameters  
564 (including both spatial and temporal abstraction multipliers), the algorithm has not been fully  
565 converged after 200000 model evaluations. This corresponds with around 19 days with an  
566 average of 8 seconds per simulation for the same processor. Of course, the evolution chain  
567 was converging towards the convergence both for the two and three-layered models. On the  
568 other hand, for the one-layered model with 57 parameters (including both spatial and  
569 temporal abstraction multipliers), the algorithm started to converge after 110000 model  
570 evaluations. Because of time limitations, abstraction multipliers associated with the spatial  
571 estimation have been excluded for all the alternative models in this study to have successful  
572 convergence results for all the models. However, we believe that this will not restrict the  
573 applicability of the approach because of the continuous advances in computational power.

574 Finally, in the third scenario, which we will refer to as IBMUEF in this study, conceptual  
575 model uncertainties are considered along with uncertainties from the model input, parameters  
576 and heteroscedasticity of groundwater level error. The IBMUEF framework is used to  
577 quantify all the mentioned sources of uncertainty in this scenario.

578 All the conceptual models have been calibrated and validated respectively for 1990 and 2000,  
579 for 12 monthly periods using 50 observation wells data for each period. It has been observed  
580 that models are able to accurately predict observation data which have not been used during  
581 the calibration. However, to ensure clear visualization, the results of 1990 are presented in the  
582 manuscript.

583 The d-factor, the % of observations within the 95 % confidence intervals (95% CI) and the  
584 Root Mean Square Error (RMSE) have been used to evaluate the model prediction  
585 uncertainty. The d-factor represents the average width of the 95% CI and is calculated as in  
586 (Yang et al., 2008):

$$d - factor = \frac{\frac{1}{n} \sum_{t=1}^n (H_{t,u} - H_{t,l})}{\sigma_0} \quad (12)$$

587 Where  $H_{t,u}$  and  $H_{t,l}$  represent respectively, the upper and lower bounds of the 95% confidence  
588 intervals,  $n$  = the number of observations and  $\sigma_0$  = the standard deviation of the observed  
589 groundwater level. d-factors closer to 1 indicate better model prediction (Yang et al., 2008).  
590 The higher observation coverage within the 95 % confidence intervals and decreasing d-  
591 factor value are indicating the improvement in model predictions and accuracy of the  
592 uncertainty bounds.

### 593 **3. Results and discussion**

594 In the results and discussion section, the results obtained from the three different scenarios as  
595 explained in the previous section (section 2.7) are presented, interpreted and discussed.  
596 Section 3.1 presents the parameter and prediction uncertainty of different conceptual models  
597 due to uncertainty of model parameters along with the heteroscedastic error model  
598 parameters. Section 3.2 elaborates on the parameter and prediction uncertainty of different  
599 conceptual models due to the uncertain input, model parameters along with the  
600 heteroscedastic error model parameters. Finally, section 3.3 presents the prediction  
601 uncertainty due to uncertainty of the conceptual model structure, input, model parameters and  
602 parameters of the heteroscedastic error model.

#### 603 **3.1 Parameter and prediction uncertainty of different conceptual models for scenario 1**

604 Figure 3 shows the posterior probability distributions of the LIB5 model parameters for  
605 scenario 1. All parameters except riverbed hydraulic conductance (RIVC) of LIB5 model are  
606 well identified within their prior distribution. The posterior distribution of RIVC is still

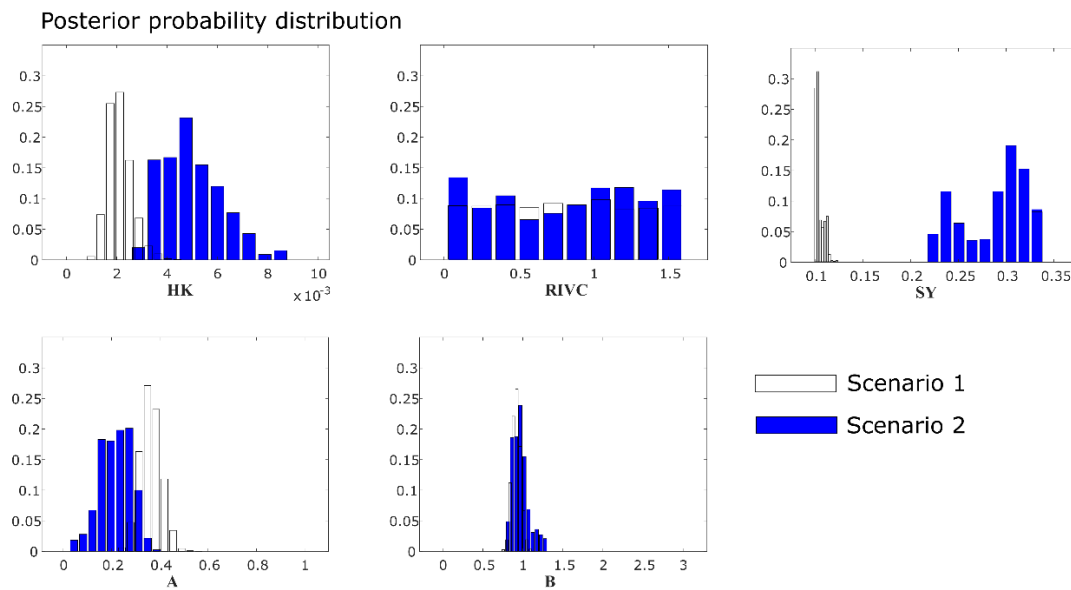
607 almost uniform while the posterior distribution of all other parameters is normally distributed,  
608 indicating that RIVC is a non-influential parameter. However, this could be improved in  
609 future studies by including more streamflow data during model calibration. We have also  
610 examined the correlation between model parameters and error model parameters. The results  
611 show a weak correlation among the MODFLOW parameters and between model parameters  
612 and error model parameters. The posterior distribution of SY is located at the lower  
613 boundaries of the prior range with a mean value of around 0.11. Alternatively, the posterior  
614 distribution of horizontal hydraulic conductivity (HK) is almost normally distributed with a  
615 high mean value of around  $2.5 \times 10^{-3} \text{ ms}^{-1}$ . However, different conceptual models with  
616 different parameterization might draw different conclusions. Hence, consideration of  
617 conceptual model structural uncertainties may be important, but this is not considered in this  
618 scenario. Although the posterior probability distributions of the well identified parameters  
619 cover only a small range of their prior distributions, the parameter uncertainty band covers  
620 only 8.5% of the observations (Figure 5a). This can be argued as a problem of  
621 overconfidence in the estimation of the model parameters. Though the total uncertainty band  
622 covers almost all observations (94%), the width of the total uncertainty band is very wide  
623 compared to the width of the parameter uncertainty band. This is indicating that both the  
624 considered conceptual model structure and the input data used for this scenario contain a  
625 considerable amount of uncertainty.

626 Figure 4 shows the posterior pdfs of the L3B5 model parameters for scenario 1. As expected,  
627 the posterior parameter distributions of the L3B5 model are very different from the posterior  
628 parameter distributions of the L1B5 model. In this scenario, 12 parameters are considered,  
629 including two parameters of the heteroscedastic error model (A and B). Out of these 12  
630 parameters, the posterior distributions of six parameters (HK-1, HK-2, HK-3, SY-1, a, and b)  
631 are approximately normally distributed. The posterior distribution of riverbed hydraulic  
632 conductance (RIVC) is still almost uniform like its prior distribution, again indicating that  
633 RIVC is a non-influential parameter. The posterior distributions of specific storage 1, 2 and 3  
634 (SS-1, SS-2 and SS-3) are not included in the figure as the posterior distributions of those  
635 parameters are also still almost uniform as were their prior distributions. Similarly, the  
636 posterior distributions of specific storage for the two layered models also remain uniform,  
637 indicating that this is also a non-influential parameter (supplementary materials:  
638 Supplementary Figure 1). The posterior distributions of HK-1 and SY-2 are located  
639 respectively at the lower and upper boundaries of the prior range. Moreover, the posterior



640 distribution of SY-3 is not well identified. This could be due to input uncertainties and/or  
 641 conceptual model structural uncertainties which are not considered in this scenario. It also  
 642 shows that the posterior probability distributions of the well identified parameters cover only  
 643 a small range of their prior distributions except for HK-2. The parameter uncertainty band  
 644 covers only 13 % of the observations (Figure 5d). Similar results are observed for the L2B4  
 645 and L2B5 models. For the L2B4 and L2B5 models, the parameter uncertainty band covers  
 646 respectively 12 % and 13.8 % of the observations (Figure 5b, 5c and Supplementary Table 1).  
 647 In general, the parameter uncertainty band is increasing with the level of complexity of the  
 648 conceptual models. The observation coverage of the parameter uncertainty band for the  
 649 different conceptual model structures is different. This suggests the importance of the use of  
 650 multiple conceptual models for reliable prediction. Hoge et al. (2019) also suggested that  
 651 consideration of uncertainty arising from conceptual physical interpretation is important  
 652 during BMA implementation, if the objective of the study is to increase the reliability and  
 653 accuracy of the model prediction.

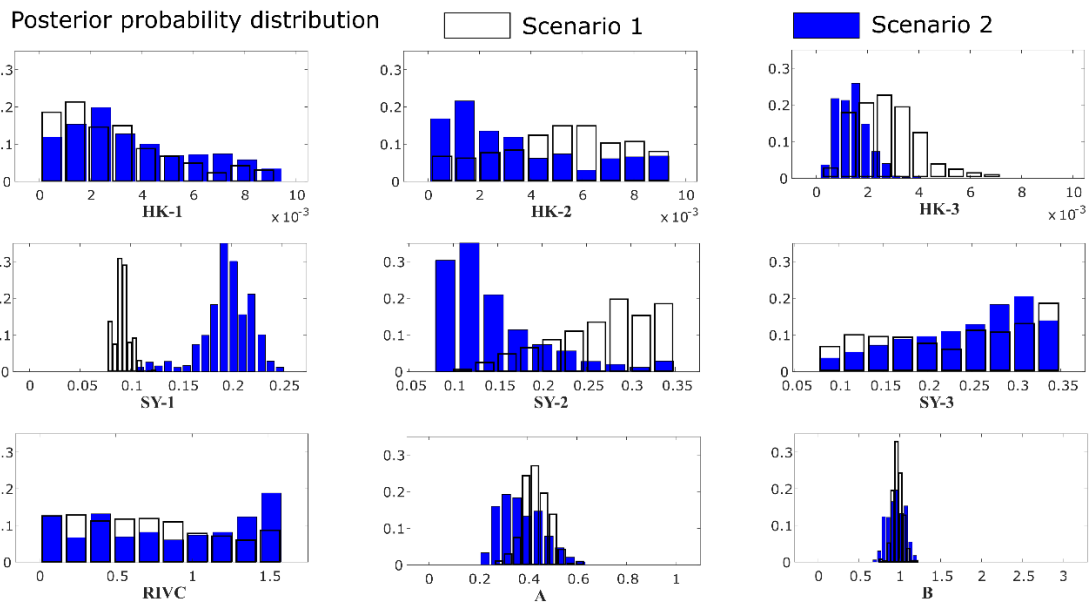
654



655

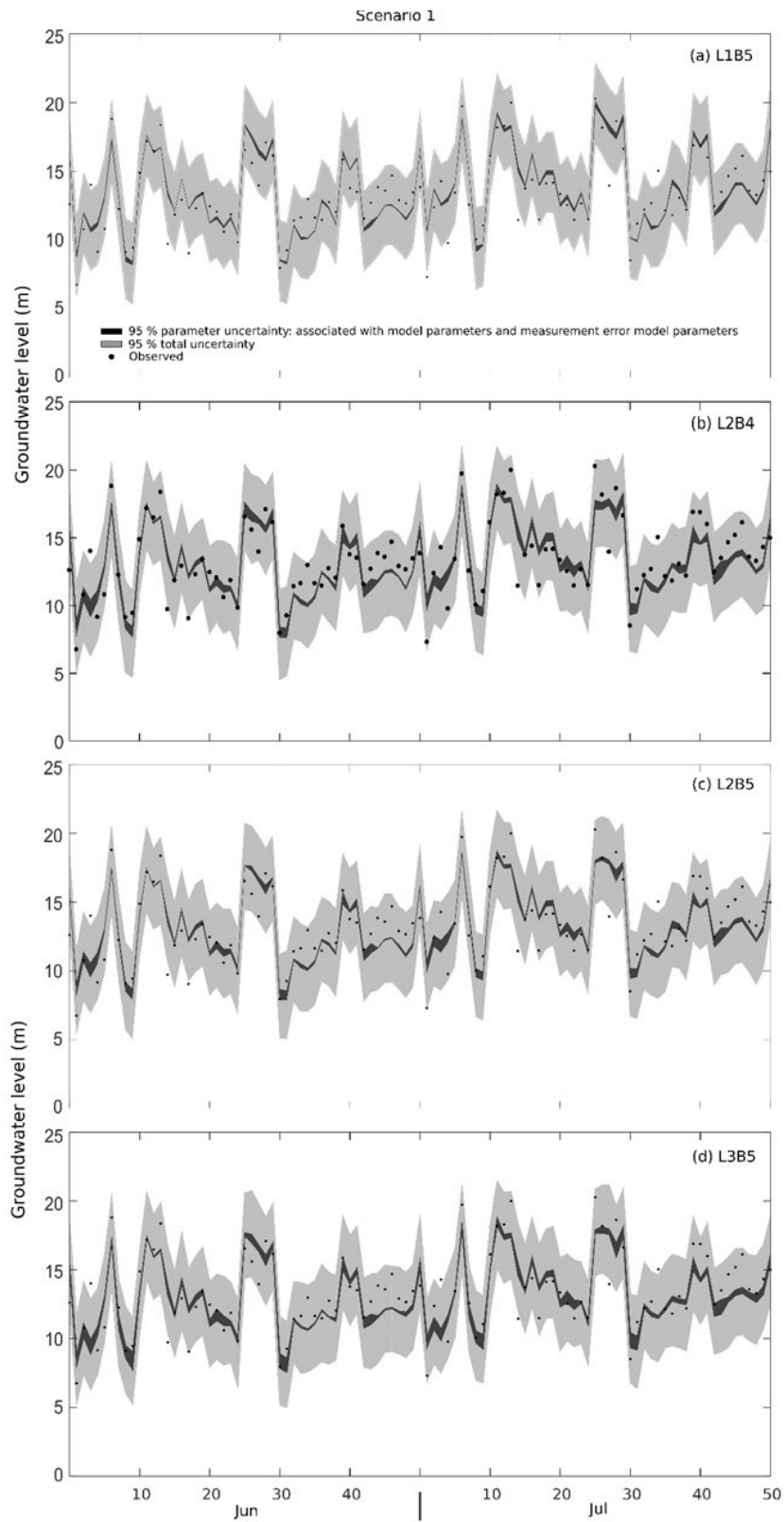
656 Figure 3: The posterior probability distribution of the L1B5 model parameters (top row) and  
 657 the parameters of the heteroscedastic error-model (bottom row) both for scenario 1 and 2,  
 658 using 2500 samples generated after convergence. HK: Horizontal hydraulic conductivity,  
 659 RIVC: Hydraulic conductance of riverbed, SY: Specific yield, A and B: The parameters of  
 660 the heteroscedastic error model.

661



662

663 Figure 4: The posterior probability distribution of the L3B5 model parameters and the  
 664 parameters of the heteroscedastic error-model (A and B) both for scenario 1 and 2, using  
 665 2500 samples generated after convergence.



666

667 Figure 5: The prediction uncertainty of monthly groundwater level at each observation well  
 668 with 95% parameter uncertainty considering error-model parameter along with model  
 669 parameter (black interval), 95 % total uncertainty (dark gray) and observations (black dot) for  
 670 (a) L1B5 model, (b) L2B4 model, (c) L2B5 model and (d) L3B5 model.

671

### 672 **3.2 Parameter and prediction uncertainty of different conceptual models for scenario 2**

673 In this scenario, uncertainty of the input data is quantified simultaneously along with model  
674 parameters and heteroscedastic error-model parameters.

675 Figure 3 shows the posterior pdfs of the L1B5 model parameters for scenario 2. As in  
676 scenario 1, all parameters are well identified within their prior ranges except RIVC. The  
677 posterior pdfs of the well identified parameters cover only a limited part of the prior range.  
678 The posterior distribution of the hydraulic conductance of riverbed (RIVC) is still almost  
679 uniform. Additionally, the posterior distribution of SY shows a slight multimodality. The  
680 correlation among model parameters and the correlation between model parameters, error  
681 model parameters and input multipliers have been examined. The results show a weak  
682 correlation among the MODFLOW parameters and between model parameters, error model  
683 parameters and input multipliers (recharge and abstraction multipliers).

684 Out of the 12 parameters for model L3B5, the posterior distributions of eight parameters  
685 (HK-1, HK-2, HK-3, SY-1, SY-2, SY-3, a, and b) are approximately normal while it was six  
686 for scenario 1 (Figure 4). The posterior distribution of RIVC, SS-1, SS-2, SS-3 are still  
687 almost uniform.

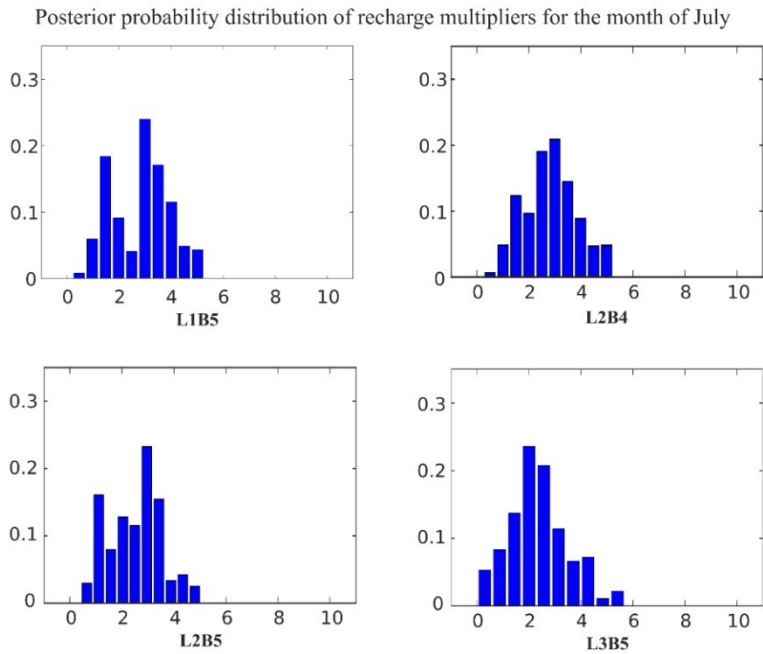
688 By comparing the posterior distributions between scenario 1 and 2 for different conceptual  
689 models (Figures 3 and 4), the following observations are made:

- 690 1. The posterior pdfs of some parameters are different in different conceptual models as  
691 well as in different scenarios. This is indicating that parameter values are overly  
692 adjusted to compensate for existing conceptual model structural deficiencies and input  
693 uncertainty when input and/or conceptual model uncertainties are not considered.
- 694 2. For model L3B5, the posterior pdfs of the parameters SY-2 and SY-3 are also  
695 identified within their prior ranges and their posterior distribution became  
696 approximately normal when we consider input uncertainty in addition to uncertainty  
697 arising from model parameters and heteroscedastic error model parameters. However,  
698 their posterior distributions are located at the boundaries of the prior range. This could  
699 be because of model structural uncertainties.
- 700 3. The heteroscedastic error model parameters (A and B) are well identified in both  
701 scenarios for all different conceptual models, but their values are different between

702 scenarios and between models. In general, the values of the error heteroscedasticity  
703 (A and B) parameters decrease when we consider input uncertainty in addition to  
704 uncertainty of model parameter and heteroscedastic error model parameters. Another  
705 important observation is that the value of the first error heteroscedasticity (A)  
706 parameter increases with the level of complexity of the conceptual models. This  
707 indicates that existing conceptual model structural deficiencies are somehow  
708 compensated by the value of the error heteroscedasticity (a) parameter.

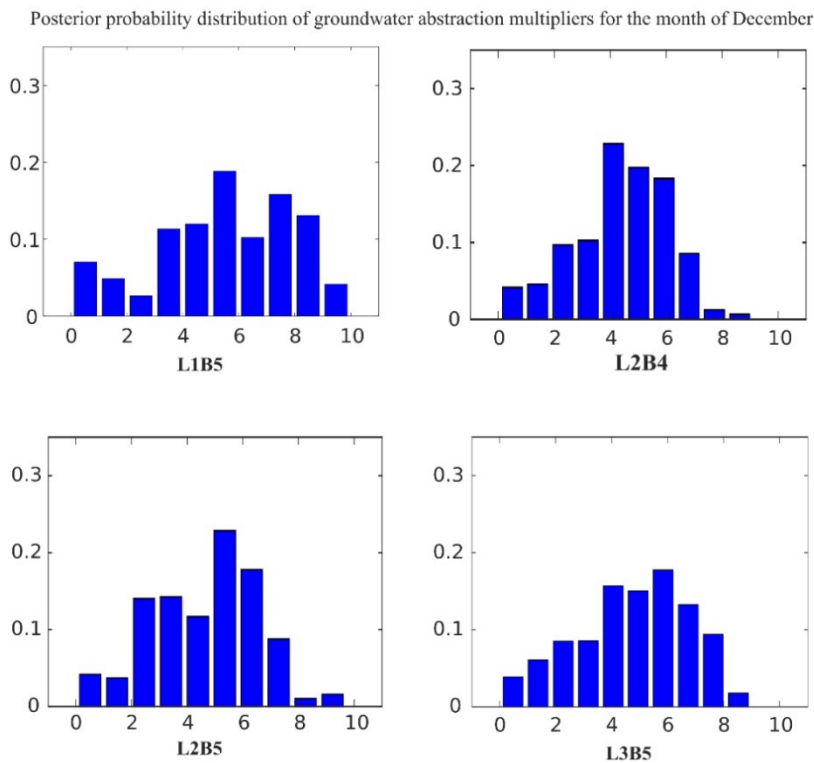
709 We conclude that an explicit consideration of input uncertainty in addition to uncertainty of  
710 the model parameters and heteroscedastic error model parameters is very important to have  
711 unbiased and better defined parameter sets. Consideration of alternative conceptual models is  
712 also important for obtaining confident parameter sets. Schoniger et al. (2015) also reported  
713 that consideration of uncertainty arising from the model input is necessary to increase the  
714 robustness of Bayesian model averaging and ranking.

715 The posterior probability distributions of the recharge multipliers vary strongly between  
716 months, but are in general higher than one. The recharge multipliers are well identified during  
717 the rainy season (May to October), while these multipliers are not well identifiable during the  
718 dry season (November to April). The details of the recharge multipliers for a specific  
719 conceptual model are explained in Mustafa et al. (2018). The distributions of the well  
720 identified multipliers show different shapes for different conceptual models (Figure 6).  
721 However, the range of the multipliers and magnitude of their probability distributions are the  
722 same for different conceptual models (Figure 6). The groundwater abstraction multipliers are  
723 also well identified within their prior range and are higher than one in all months except for  
724 November and January for all four conceptual models. Again, the well identified multipliers  
725 show almost the same range of values for different conceptual models (Figure 7). This  
726 indicates that the input uncertainty multipliers are independent from model structural  
727 uncertainty and are not overly adjusted to compensate conceptual model structural  
728 deficiencies.



729

730 Figure 6: Posterior distribution of groundwater recharge multipliers of July for all conceptual  
 731 models, using 2500 samples generated after convergence.

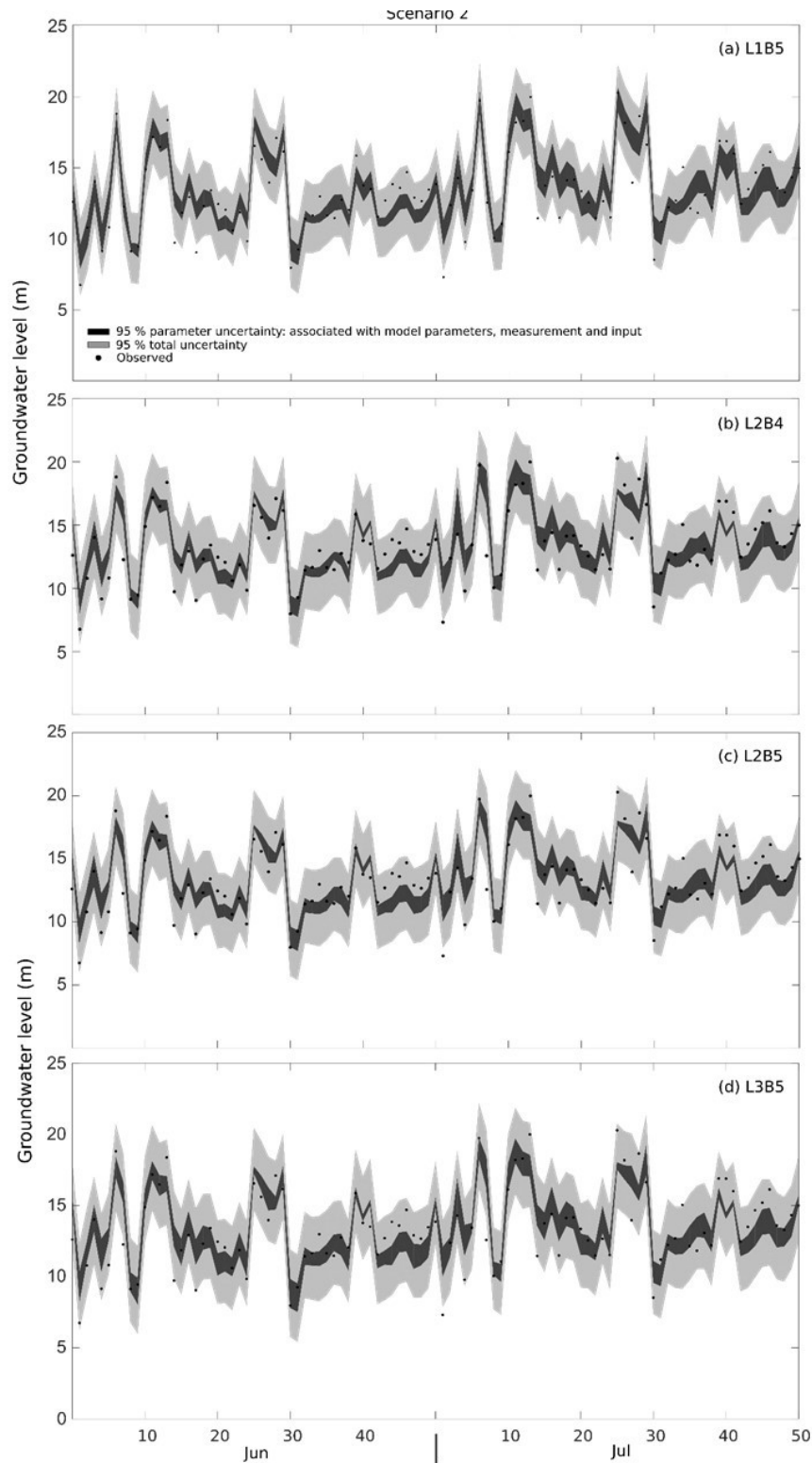


732

733 Figure 7: Posterior distribution of groundwater abstraction multipliers, using 2500 samples  
 734 generated after convergence.

735

736 The prediction uncertainty of the monthly groundwater level associated with input  
737 uncertainty, model parameter uncertainty and uncertainty related to the heteroscedastic error  
738 model is presented in figure 8. The observation coverage of the parameter uncertainty band  
739 has increased by more than 100% for all models (Supplementary Table 1) when uncertainty  
740 arising from model input is incorporated along with uncertainty arising from model  
741 parameters and parameters of the heteroscedastic error model. The increase for the L1B5  
742 model is even more than 200%. This result reveals that consideration of input uncertainty has  
743 significantly improved the confidence of model predictions and ignoring input uncertainty  
744 could lead to biased model simulations and incorrect uncertainty bands.. The parameter  
745 uncertainty band of L1B5 covers the highest number of observations when input uncertainty  
746 is included (Supplementary Table 1). When we explicitly consider input uncertainty, the  
747 width of the parameter uncertainty band has increased but the width of the total uncertainty  
748 has decreased (figure 5 and 8). This indicates that total uncertainty has decreased. This is  
749 confirmed by the reduction of the d-factor for all the models (Supplementary Table 1). This  
750 result reveals that uncertainty bounds of scenario 2 are more accurate compared to the CI of  
751 scenario 1, and the residual variance is smaller at each point. The Root Mean Square Error  
752 (RMSE) was also used to compare the results of scenario 1 and 2. It is observed that the  
753 values of the RMSE are decreasing when input uncertainty is included along with model  
754 parameter uncertainty and the parameters of the heteroscedastic error model (Figure 14). The  
755 decreasing magnitude of the RMSE value of L1B5 model is more significant than for any of  
756 the other models, indicating comparatively higher uncertainties in the L1B5 model. This is  
757 another indication that consideration of uncertainties through input multipliers is increasing  
758 the accuracy of the model prediction and decreasing the prediction uncertainty. Even after  
759 consideration of input uncertainties, the observation coverage of the parameter uncertainty  
760 band for the different conceptual model structures is different (Supplementary Table 1,  
761 Figure 8). Hence, consideration of conceptual model structural and input uncertainty is  
762 important to have more accurate model prediction and unbiased uncertainty bounds.



763

764 Figure 8: Prediction uncertainty of monthly groundwater level at each observation well with  
 765 95% parameter uncertainty considering input uncertainty along with model parameter  
 766 uncertainty and error heteroscedasticity (black interval), 95 % total uncertainty (dark gray)  
 767 and observation (black dot) for (a) L1B5 model, (b) L2B4 model, (c) L2B5 model and (d)  
 768 L3B5 model.



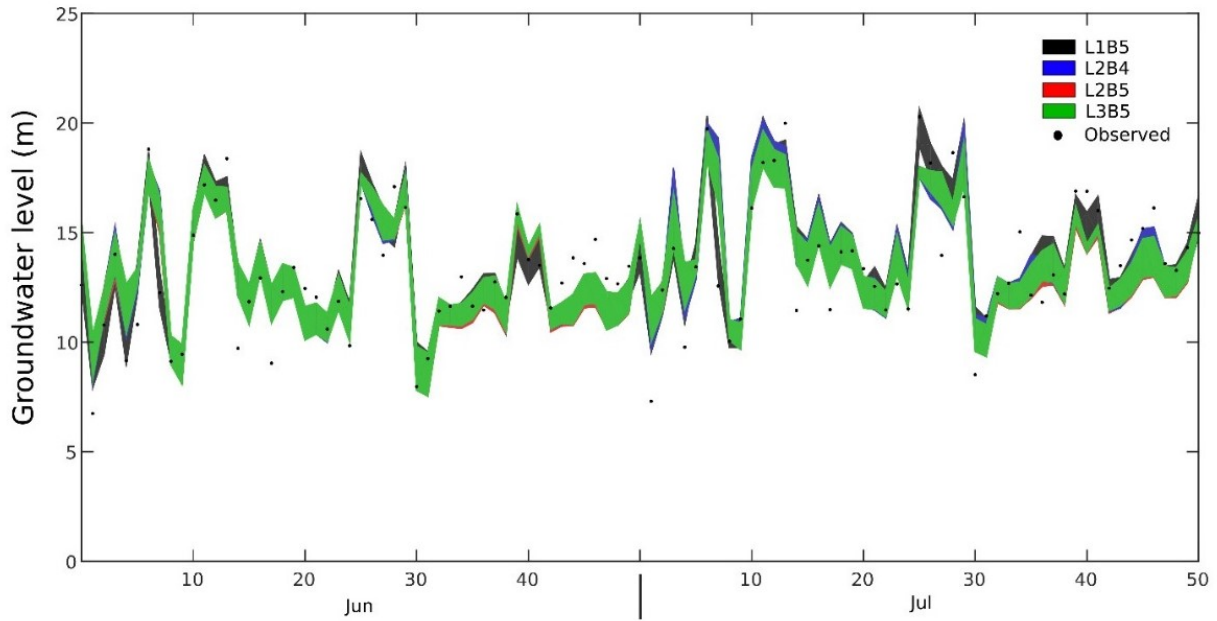
769 **3.3 Application of IBMUEF: assessment of the model uncertainty from input, model**  
770 **parameters, parameters of the heteroscedastic error-model and conceptual model**  
771 **structure**

772 In the IBMUEF framework, uncertainties originating from the model input, the parameters,  
773 the parameters of the heteroscedastic error-model and the conceptual model structure can be  
774 taken into account. In this section, besides a presentation and discussion of the results of the  
775 IBMUEF application, these are also compared with the results of the previous scenarios.

776 Figure 9 shows parameter uncertainty bounds for all four alternatives conceptual models  
777 considering uncertainty arising from model input, parameter, and measurement  
778 heteroscedasticity. The different conceptual model structures cover different observations.  
779 This is indicating the skill of the models to capture different hydrogeological processes of the  
780 system.

781 The marginal densities of the estimated weights (following step 9 of section 2.4) for each  
782 model are shown in figure 10. The weight of the L1B5 model is well identified and has a  
783 normal distribution. Its likelihood value (weight) is very high compared to other models. The  
784 weight of all other models is very small. Nevertheless, their contribution is considered in the  
785 final results as they are representing different geological processes which are not considered  
786 in L1B5. The necessity of incorporating different models is also confirmed by the limited  
787 correlations between the groundwater level predictions using different conceptual models  
788 (Supplementary Table 2). For example, if a researcher/user knows the L1B5 model  
789 prediction, the L2B5 model adds more additional information to the final result compared to  
790 the L2B4 and L3B5 models as L2B5 is less correlated with L1B5. In general, correlations  
791 between the models are limited, indicating that different conceptual models are providing  
792 important information of the different hydrogeologic processes of the system. Hence,  
793 consideration of different conceptual models is needed to have a reliable model prediction.

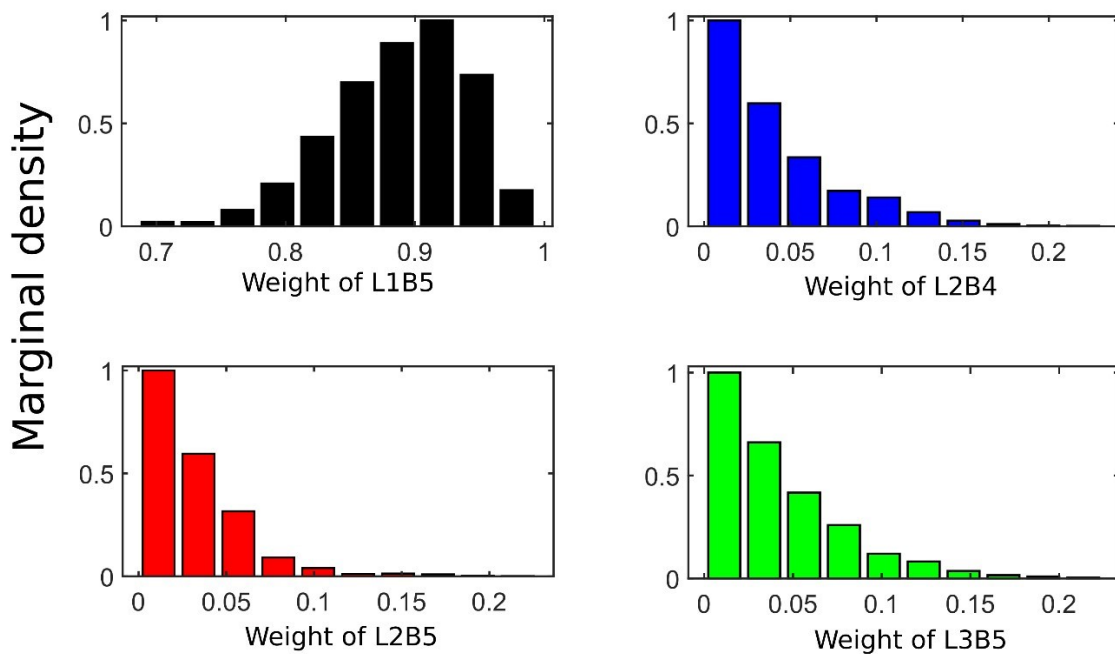
794



795

796 Figure 9: Prediction uncertainty of monthly groundwater level for all the conceptual models  
 797 at each observation well with 95% parameter uncertainty considering input uncertainty along  
 798 with model parameter uncertainty and error heteroscedasticity and observation (black dot).

799



800

801 Figure 10: Marginal density of estimated weight for each model using integrated Bayesian  
 802 multi-model uncertainty estimation framework (IBMUEF).

803

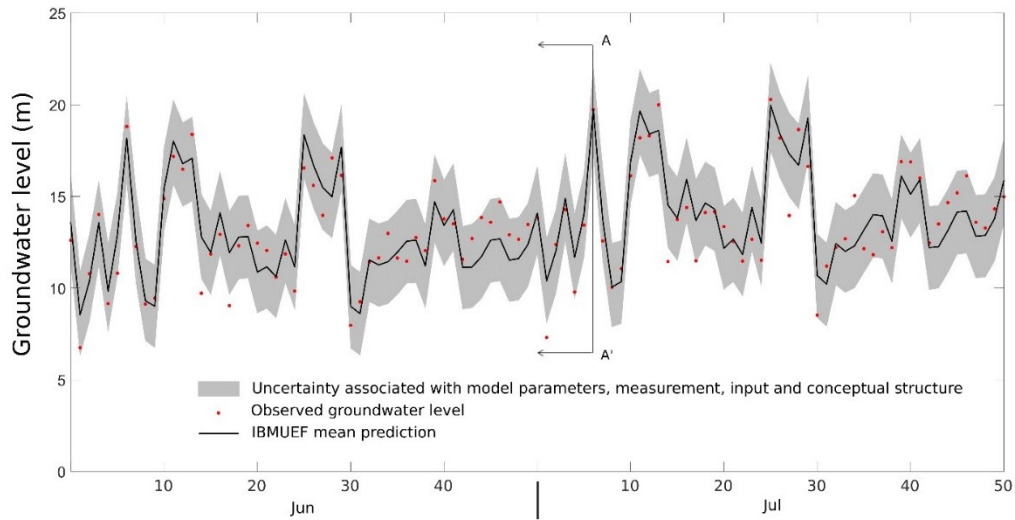
804

805 Figure 11 shows the final IBMUEF 95% prediction uncertainty of the monthly groundwater  
806 levels at each observation well considering model input, parameter, error heteroscedasticity  
807 model parameter, and conceptual model structural uncertainty. The final IBMUEF prediction  
808 was calculated using the prediction of the individual member models and their corresponding  
809 likelihood values (Figures 9 and 10) as explained in sections 2.3 and 2.4. The black line in  
810 figure 11 shows the mean prediction of the IBMUEF. The IBMUEF mean prediction and  
811 variance of figure 11 were calculated using equation 7 and 8, respectively. The distribution  
812 shape is determined by the weighted sum of the posterior distributions of each member model  
813 (Figure 12). It is observed that the posterior distribution of L1B5 model is capturing the  
814 reality more accurately compared to other models in the selected section of figure 11 (Figure  
815 12). Hence, the distribution shape of the L1B5 model has a dominant role on the final  
816 IBMUEF prediction distribution shape of that section.

817 As expected, the 95 % CI of IBMUEF covers 95% of the observations which is very high  
818 compared to the individual models (Figure 11 and 13). Another interesting observation is that  
819 the d-factor value (1.42) has become smaller than the previous results. This is an indication of  
820 the improved model predictions and accuracy of the uncertainty bounds. The Root Mean  
821 Square Error (RMSE) was also used to evaluate the skill of the IBMUEF and to compare it  
822 with the individual model ensembles. The probability distributions of the RMSE-values for  
823 each of the models and IBMUEF are shown in figure 14. It is observed that the IBMUEF  
824 results in lower RMSE values compared to any individual model from the ensemble (Figure  
825 14). This result reveals that the IBMUEF framework provides better model predictions. We  
826 conclude that an explicit consideration of conceptual model structural uncertainty is  
827 important for obtaining more accurate model predictions and unbiased uncertainty bounds.  
828 The results for this study are in line with results from similar approaches in surface water  
829 modeling (e.g., Ajami et al., 2007).

830 The IBMUEF framework is providing better and more reliable model predictions and more  
831 accurate uncertainty bounds, which is very important for decision support applications.  
832 However, as mentioned earlier, the implementation of the methodology is computationally  
833 expensive. The computational burden has also been identified as a main drawback for all  
834 other existing integrated uncertainty assessment approaches (Rojas et al., 2008; Ajami et al.,  
835 2007; Gelman et al., 2014). Based on their hypothetical setup, Xue & Zhang (2014) and

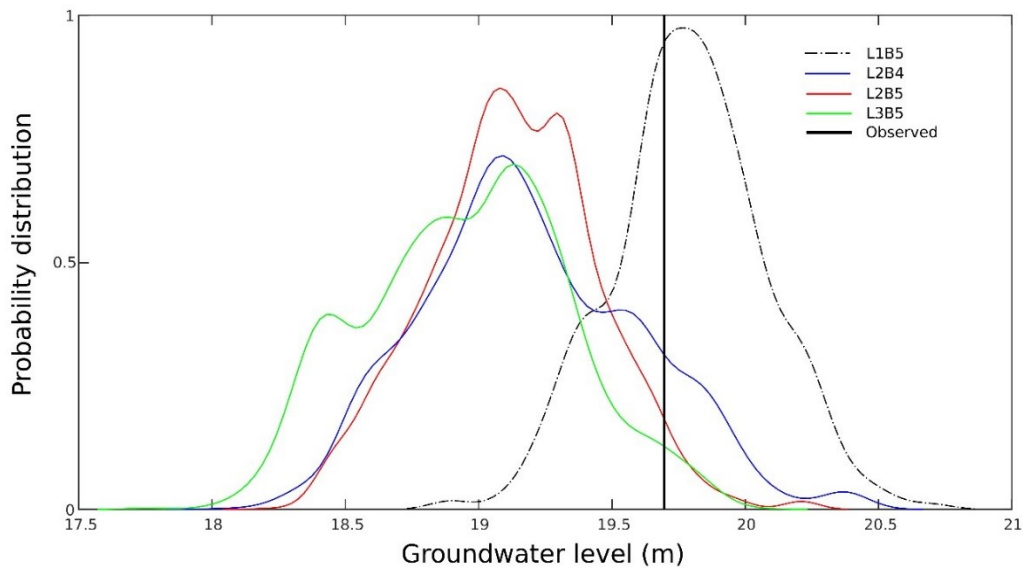
836 Hendricks Franssen et al. (2011) advocated that the EnKF is computationally more efficient  
837 compared to other existing Bayesian methods. However, comparison of the computational  
838 efficiency of the EnKF and other integrated Bayesian approaches with a real-world model  
839 remain unsolved. Another alternative could be Granger-Ramanathan averaging (GRA). GRA  
840 provides very similar performance as BMA, but is computationally less demanding (Diks and  
841 Vrugt, 2010). The information criterion (e. g.: AIC: Akaike information criterion) is another  
842 alternative to obtain a computationally less demanding approach (Hoge et al. 2019).  
843 However, model averaging based on AIC has been criticised by researchers as it is not based  
844 on a rigorous statistical basis and its results has no BMA interpretation (Wasserman, 2000;  
845 Tsai and Elshall, 2013). That's why it has been considered as a model selection technique  
846 instead of model averaging (Hoge et al. 2019). As a consequence, we have to choose between  
847 two different approaches: (i) computationally demanding but statistically robust, reliable and  
848 more accurate approaches or (ii) approaches without rigorous statistical foundation, which are  
849 computationally less demanding. Nonetheless, the statistically robust adaptive MCMC  
850 sampling of the DREAM algorithm is computationally more efficient for high-dimensional  
851 and multimodal application (Vrugt et al 2009a, 2016; Leta et al., 2015). Since the latter multi-  
852 chain MCMC based algorithm has been adopted in this study as a sampling approach, we  
853 believe that our approach is computationally more efficient compared to other existing  
854 integrated uncertainty assessment approaches. Moreover, the IBMUEF is a flexible  
855 framework as (i) there is no limitation for the number or complexity of alternative conceptual  
856 models and (ii) users can choose the number and dimensions (spatial and temporal) of input  
857 multipliers, based on the objectives of their modelling. It should be remembered that, the  
858 computational time increases with increases complexity of the alternative conceptual  
859 groundwater models and for a very complex model with more than 60 model parameters, the  
860 proposed approach became computationally very expensive. However, we believe that this  
861 will not restrict the applicability of the approach because of the continuous advances in  
862 computational power. Even though, effort should continue in the development of a more  
863 computationally efficient approach. We conclude that number or complexity of alternative  
864 conceptual models should be considered based on the modelling objectives during the  
865 implementation of a integrated uncertainty assessment approaches. Hoge et al. (2019) also  
866 concluded that the objective of the modelling should be the main driver in selecting model  
867 averaging approaches.



868

869 Figure 11: 95 % prediction uncertainty of monthly groundwater level at each observation  
 870 well considering model input, parameter, error heteroscedasticity model parameter, and  
 871 conceptual model structural uncertainty (gray shad), and IBMUEF predictive mean (black  
 872 line), observation (red dot).

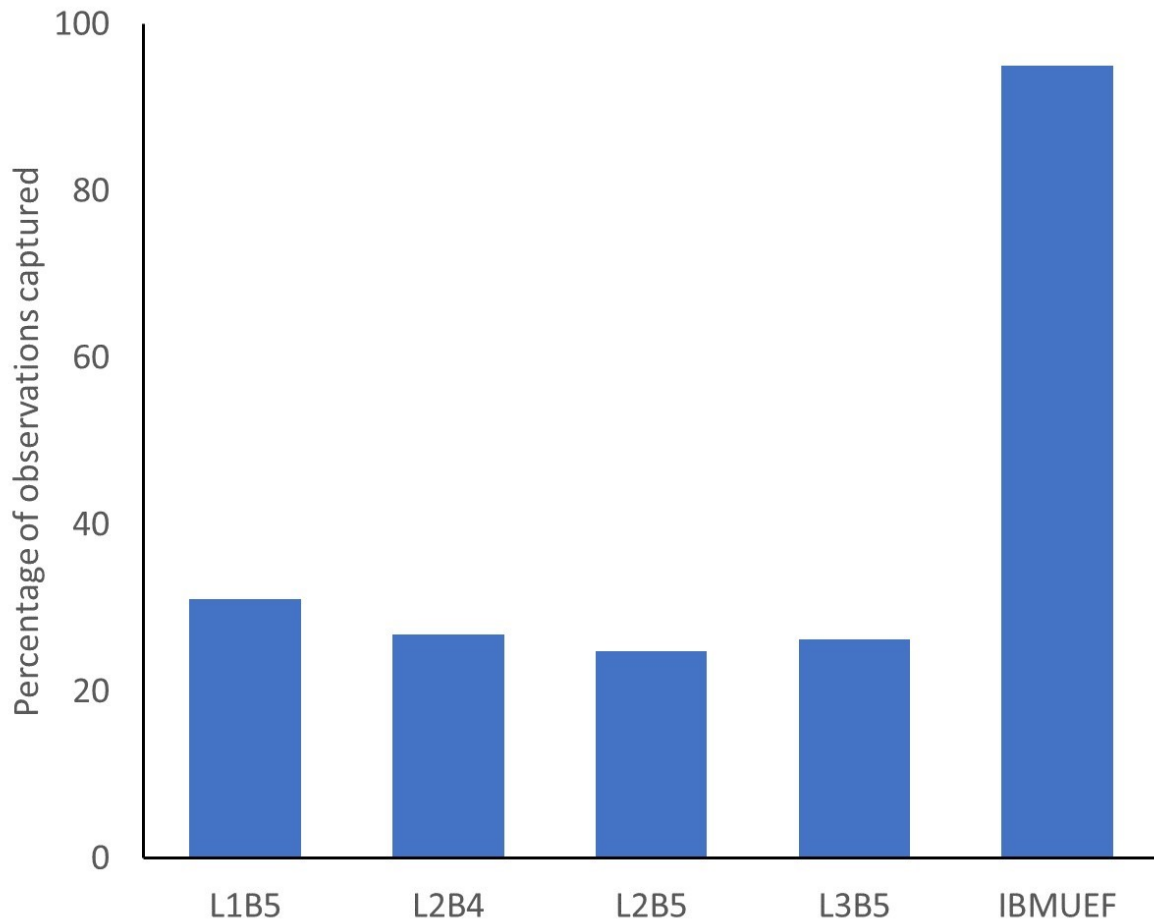
873



874

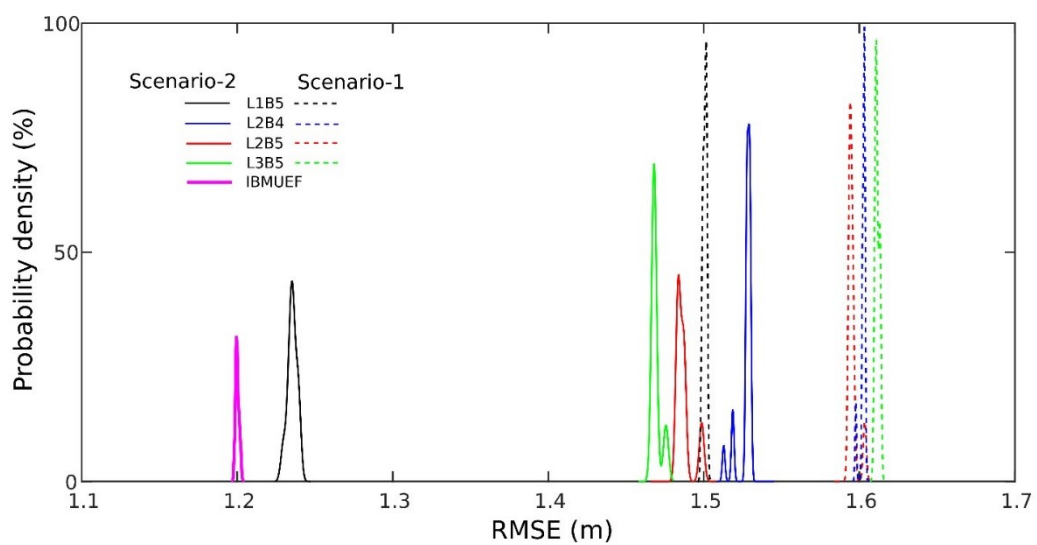
875 Figure 12: Posterior probability distribution of groundwater level prediction for each member  
 876 model at the selected cross-section (A-A') of figure 11 and observed groundwater level  
 877 (black line).

878



879  
 880 Figure 13: Percentage of observation captured by 95% parameter uncertainty bands of each  
 881 conceptual model and IBMUEF.

882



883  
 884 Figure 14: Probability distribution of RMSE for each model both for scenario 1 and 2 and  
 885 IBMUEF.

#### 886 **4. Conclusions**

887 We present an integrated Bayesian multi-model uncertainty estimation framework (IBMUEF)  
888 to explicitly quantify the uncertainty originating from errors in model conceptualization,  
889 input data, parameter values and measurement heteroscedasticity error of a fully distributed  
890 physically-based groundwater flow model. In the proposed integrated fully Bayesian multi-  
891 model framework, the DREAM algorithm with a specific likelihood function is combined  
892 with BMA. Groundwater recharge multipliers and groundwater abstraction multipliers are  
893 used in this framework to quantify uncertainty of spatially distributed input data of the  
894 groundwater model. The measurement heteroscedasticity is also considered in our integrated  
895 Bayesian framework by incorporating a novel heteroscedastic error model. To check the  
896 applicability of IBMUEF, four alternative conceptual models have been developed using a  
897 numerical groundwater flow model (MODFLOW) based on different interpretations of  
898 geological and hydrogeological information about the study area.

899 The results of this study confirm that conceptual model structure and uncertainty on the input  
900 data have a considerable effect on the model parameter distributions and model predictions.  
901 We demonstrated that parameter values are overly adjusted to compensate the existing  
902 conceptual model structural deficiencies and input uncertainty when they are not taken into  
903 account. Although consideration of input uncertainty results in better defined parameter  
904 distributions, consideration of alternatives conceptual models is also important to obtain  
905 confident parameter sets as the existing conceptual model structural deficiencies are  
906 somehow compensated by parameter uncertainties and the parameters of the heteroscedastic  
907 error model. On the other hand, input uncertainty multipliers appear to be independent from  
908 model structural uncertainty.

909 The total uncertainty of the system decreases but the observation coverage of the parameter  
910 uncertainty band increases by more than 100 % for all considered models when input  
911 uncertainty is included. Even when considering input uncertainty, the observation coverage  
912 of the parameter uncertainty band for the different conceptual model structures is different.  
913 This suggests the importance of the use of multiple conceptual models for reliable prediction.  
914 The parameter uncertainty band of L1B5 covers the highest number of observations when  
915 input uncertainty is included. This indicates that the L1B5 model is more capable of  
916 capturing the reality when input uncertainty is included. This is also confirmed by the highest  
917 likelihood (weight) value of the model. We demonstrate that consideration of input

918 uncertainty along with model parameters uncertainty and measurement error generate more  
919 reliable model predictions. However, a very common limitation of these results is that the  
920 results are based on only a single conceptual model. Our results also confirm that even a very  
921 well calibrated conceptual model is unable to represent all the hydrogeologic processes of the  
922 system.

923 The IBMUEF prediction was calculated using the prediction of the individual member  
924 models and their corresponding likelihood values. The 95% prediction uncertainty band of  
925 IBMUEF covers 95 % of the observations which is significantly higher compared to any of  
926 the individual models. The IBMUEF framework has decreased the RMSE-value of the  
927 prediction and d-factor of the CI, and thereby increased the reliability of the prediction. The  
928 results of the study confirm that the IBMUEF framework is a useful tool to have better and  
929 more reliable model predictions and accurate uncertainty bounds. It is also shown that the  
930 IBMUEF is a useful and applicable framework to simultaneously quantify input, parameter,  
931 measurement and conceptual model uncertainty of a fully distributed physically-based  
932 groundwater flow model. We conclude that an explicit consideration of conceptual model  
933 structural uncertainty along with model input, parameter and measurement uncertainty using  
934 IBMUEF framework improves the accuracy and reliability of the model prediction and  
935 related uncertainty bounds.

936 Alternative conceptual models considered in this study have been developed using only  
937 MODFLOW. Future studies could be conducted considering different groundwater modelling  
938 algorithms to quantify the effect of numerical modelling errors. The modified log-likelihood  
939 function as explained in section 2.2, has been used in this study. However, future studies  
940 could be conducted considering different likelihood function to evaluate the effect of  
941 likelihood function.

942 In future studies, the framework can be implemented with more additional data sets to check  
943 the applicability with different prediction objectives e.g: baseflow. Moreover, application of  
944 the IBMUEF framework to quantify the groundwater level prediction uncertainties  
945 originating from the climate change and abstraction scenarios will increase the reliability of  
946 the model prediction and accuracy of the uncertainty bounds as its (IBMUEF) already  
947 consider all the other sources of uncertainties. However, number or complexity of alternative  
948 conceptual models or future scenarios should be considered based on the modelling



949 objectives during implementation of this integrated uncertainty assessment approaches to  
950 avoid conceptual burden.

## 951 **Acknowledgments**

952 We thank Prof. Jasper Vrugt from University of California, Irvine, USA for his advice on the  
953 implementation of BMA. A draft version of a conference abstract appears online at  
954 AgEng2018.com but has not been published. The data used in this study are summarized and  
955 presented in the figures, tables, references and supporting information and will be available  
956 from the authors upon request (syed.mustafa@vub.be).

## 957 **Author contributions**

958 SM, JN and MH designed the study. SM and GG performed the analysis. SM and MH wrote  
959 the manuscript. All authors discussed the results and commented on the manuscript.

## 960 **References**

- 961 Abdollahi, K., Bashir, I., Verbeiren, B., Harouna, M. R., Van Griensven, A., Huysmans, M.  
962 & Batelaan, O. (2017). A distributed monthly water balance model: formulation and  
963 application on Black Volta Basin, *Environmental Earth Sciences*, 76(5), 198,  
964 <https://doi.org/10.1007/s12665-017-6512-1>.
- 965 Ajami, N. K., Duan, Q., & Sorooshian, S. (2007). An integrated hydrologic Bayesian  
966 multimodel combination framework: Confronting input, parameter, and model  
967 structural uncertainty in hydrologic prediction. *Water Resources Research*, 43(1).
- 968 Akaike, H. (1974). Markovian representation of stochastic processes and its application to the  
969 analysis of autoregressive moving average processes. *Annals of the Institute of*  
970 *Statistical Mathematics*, 26(1), 363–387.
- 971 Batelaan, O., & De Smedt, F. (2007). GIS-based recharge estimation by coupling surface–  
972 subsurface water balances. *Journal of Hydrology*, 337(3-4), 337-355.
- 973 Beven, K. (1993). Prophecy, reality and uncertainty in distributed hydrological modelling.  
974 *Advances in Water Resources*, 16(1), 41–51.
- 975 Beven, K., & Binley, A. (1992). The future of distributed models: model calibration and  
976 uncertainty prediction. *Hydrological Processes*, 6(3), 279–298.
- 977 Bredehoeft, J. (2005). The conceptualization model problem—surprise. *Hydrogeology*  
978 *Journal*, 13(1), 37–46.

- 979 Chitsazan, N., & Tsai, F. T. C. (2015). A hierarchical Bayesian model averaging framework  
980 for groundwater prediction under uncertainty. *Groundwater*, 53(2), 305-316.
- 981 Diks, C. G., & Vrugt, J. A. (2010). Comparison of point forecast accuracy of model  
982 averaging methods in hydrologic applications. *Stochastic Environmental Research  
983 and Risk Assessment*, 24(6), 809-820.
- 984 Doherty J. (2000), PEST - Model-independent parameter estimation. User's manual.  
985 Watermark Computing. Australia
- 986 Domenico, P. A., & Mifflin, M. D. (1965). Water from low-permeability sediments and land  
987 subsidence. *Water Resources Research*, 1(4), 563-576.
- 988 Domenico, P. A., & Schwartz, F. W. (1998). *Physical and chemical hydrogeology* (Vol. 506).  
989 Wiley New York.
- 990 Draper, D. (1994). Assessment and propagation of model uncertainty. *Journal of the Royal  
991 Statistical Society, Series B*, 56.
- 992 Elshall, A. S., & Tsai, F. T. C. (2014). Constructive epistemic modeling of groundwater flow  
993 with geological structure and boundary condition uncertainty under the Bayesian  
994 paradigm. *Journal of Hydrology*, 517, 105-119.
- 995 Enemark, T., Peeters, L. J., Mallants, D., & Batelaan, O. (2019). Hydrogeological conceptual  
996 model building and testing: A review. *Journal of hydrology*, 569, 310-329.
- 997 Gaganis, P., & Smith, L. (2006). Evaluation of the uncertainty of groundwater model  
998 predictions associated with conceptual errors: A per-datum approach to model  
999 calibration. *Advances in Water Resources*, 29(4), 503-514.
- 1000 Gelman, A., Hwang, J., & Vehtari, A. (2014). Understanding predictive information criteria  
1001 for Bayesian models. *Statistics and computing*, 24(6), 997-1016.
- 1002 Gupta, H. V., Clark, M. P., Vrugt, J. A., Abramowitz, G., & Ye, M. (2012). Towards a  
1003 comprehensive assessment of model structural adequacy. *Water Resources Research*,  
1004 48(8).
- 1005 Hendricks Franssen, H. J., Kaiser, H. P., Kuhlmann, U., Bauser, G., Stauffer, F., Müller, R.,  
1006 & Kinzelbach, W. (2011). Operational real-time modeling with ensemble Kalman  
1007 filter of variably saturated subsurface flow including stream-aquifer interaction and  
1008 parameter updating. *Water resources research*, 47(2).
- 1009 Hill, M. C., & Tiedeman, C. R. (2007). Effective groundwater model calibration: with  
1010 analysis of data, sensitivities, predictions, and uncertainty. John Wiley & Sons.
- 1011 Hoeting, J. A., Madigan, D., Raftery, A. E., & Volinsky, C. T. (1999). Bayesian model  
1012 averaging: a tutorial. *Statistical Science*, 382-401.

- 1013 Höge, M., Guthke, A., & Nowak, W. (2019). The Hydrologist's Guide to Bayesian Model  
1014 Selection, Averaging and Combination. *Journal of Hydrology*, 572, 96-107.
- 1015 Højberg, A. L., & Refsgaard, J. C. (2005). Model uncertainty–parameter uncertainty versus  
1016 conceptual models. *Water Science and Technology*, 52(6), 177–186.
- 1017 Johnson, A. I. (1967). *Specific yield: compilation of specific yields for various materials*. US  
1018 Government Printing Office.
- 1019 Johnson, R. H. (2007). Ground water flow modeling with sensitivity analyses to guide field  
1020 data collection in a mountain watershed. *Groundwater Monitoring & Remediation*,  
1021 27(1), 75-83.
- 1022 Kavetski, D., Kuczera, G., & Franks, S. W. (2006a). Bayesian analysis of input uncertainty in  
1023 hydrological modeling: 1. Theory. *Water Resources Research*, 42.
- 1024 Kavetski, D., Kuczera, G., & Franks, S. W. (2006b). Bayesian analysis of input uncertainty in  
1025 hydrological modeling: 2. Application. *Water Resources Research*, 42(3).
- 1026 Kuczera, G., Kavetski, D., Franks, S., & Thyer, M. (2006). Towards a Bayesian total error  
1027 analysis of conceptual rainfall-runoff models: Characterising model error using storm-  
1028 dependent parameters. *Journal of Hydrology*, 331(1), 161–177.
- 1029 Laloy, E., Rogiers, B., Vrugt, J. A., Mallants, D., & Jacques, D. (2013). Efficient posterior  
1030 exploration of a high-dimensional groundwater model from two-stage Markov chain  
1031 Monte Carlo simulation and polynomial chaos expansion. *Water Resources Research*,  
1032 49(5), 2664-2682.
- 1033 Leta, O. T., Nossent, J., Velez, C., Shrestha, N. K., van Griensven, A., & Bauwens, W.  
1034 (2015). Assessment of the different sources of uncertainty in a SWAT model of the  
1035 River Senne (Belgium). *Environmental Modelling & Software*, 68, 129-146.
- 1036 Li, X., & Tsai, F. T.-C. (2009). Bayesian model averaging for groundwater head prediction  
1037 and uncertainty analysis using multimodel and multimethod. *Water Resources  
1038 Research*, 45(9).
- 1039 Madigan, D., Raftery, A. E., Volinsky, C., & Hoeting, J. (1996). Bayesian model averaging,  
1040 in *Proceedings of the AAAI Workshop on Integrating Multiple Learned Models* (pp.  
1041 77–83). AAAI Press, Portland, Oreg.
- 1042 Mantovan, P., & Todini, E. (2006). Hydrological forecasting uncertainty assessment:  
1043 Incoherence of the GLUE methodology. *Journal of Hydrology*, 330(1), 368–381.
- 1044 Michael, H. A., & Voss, C. I. (2009a). Controls on groundwater flow in the Bengal Basin of  
1045 India and Bangladesh: regional modeling analysis. *Hydrogeology Journal*, 17(7),  
1046 1561.

- 1047 Michael, H. A., & Voss, C. I. (2009b). Estimation of regional-scale groundwater flow  
1048 properties in the Bengal Basin of India and Bangladesh. *Hydrogeology Journal*, 17(6),  
1049 1329–1346.
- 1050 Minka, T. P. (2002). Bayesian model averaging is not model combination. Available  
1051 electronically at <http://www.stat.cmu.edu/minka/papers/bma.html>, 1-2.
- 1052 Montanari, A. (2005). Large sample behaviors of the generalized likelihood uncertainty  
1053 estimation (GLUE) in assessing the uncertainty of rainfall-runoff simulations. *Water*  
1054 *Resources Research*, 41(8).
- 1055 Monteith, K., Carroll, J. L., Seppi, K., & Martinez, T. (2011, July). Turning Bayesian model  
1056 averaging into Bayesian model combination. In *The 2011 International Joint*  
1057 *Conference on Neural Networks* (pp. 2657-2663). IEEE.
- 1058 Mustafa, S. M. T., Nossent, J., Ghysels, G., & Huysmans, M. (2018). Estimation and Impact  
1059 Assessment of Input and Parameter Uncertainty in Predicting Groundwater Flow with  
1060 a Fully Distributed Model. *Water Resources Research*, 54(9), 6585-6608, doi:  
1061 10.1029/2017WR021857.
- 1062 Mustafa, S. M. T., Abdollahi, K., Verbeiren, B., & Huysmans, M. (2017a). Identification of  
1063 the influencing factors on groundwater drought and depletion in north-western  
1064 Bangladesh. *Hydrogeology Journal*, 25(5), 1357–1375.
- 1065 Mustafa, S. M. T., Vanuytrecht, E., & Huysmans, M. (2017b). Combined deficit irrigation  
1066 and soil fertility management on different soil textures to improve wheat yield in  
1067 drought-prone Bangladesh. *Agricultural Water Management*, 191, 124-137.
- 1068 Mustafa, S. M. T., Hasan, M. M., Saha, A. K., Rannu, R. P., Van Uytven, E., Willems, P., &  
1069 Huysmans, M. (2019). Multi-model approach to quantify groundwater level  
1070 prediction uncertainty using an ensemble of global climate models and multiple  
1071 abstraction scenarios. *Hydrology and Earth System Sciences*, 23(5), 2279-2303,  
1072 <https://doi.org/10.5194/hess-23-2279-2019>.
- 1073 Nettasana, T., Craig, J., & Tolson, B. (2012). Conceptual and numerical models for  
1074 sustainable groundwater management in the Thaphra area, Chi River Basin, Thailand.  
1075 *Hydrogeology Journal*, 20(7), 1355–1374.
- 1076 Neuman, S. (2003). Maximum likelihood Bayesian averaging of uncertain model predictions.  
1077 *Stochastic Environmental Research and Risk Assessment*, 17(5), 291–305.
- 1078 Peeters, L. J. M., & Turnadge, C. (2019). When to account for boundary conditions in  
1079 estimating hydraulic properties from head observations?. *Groundwater*, 57(3), 351-  
1080 355.

- 1081 Poeter, E., & Anderson, D. (2005). Multimodel ranking and inference in ground water  
1082 modeling. *Groundwater*, 43(4), 597–605.
- 1083 Raftery, A. E., Gneiting, T., Balabdaoui, F., & Polakowski, M. (2005). Using Bayesian model  
1084 averaging to calibrate forecast ensembles. *Monthly Weather Review*, 133(5), 1155–  
1085 1174.
- 1086 Refsgaard, J. C., Van der Sluijs, J. P., Brown, J., & Van der Keur, P. (2006). A framework for  
1087 dealing with uncertainty due to model structure error. *Advances in Water Resources*,  
1088 29(11), 1586–1597.
- 1089 Refsgaard, J. C., van der Sluijs, J. P., Højberg, A. L., & Vanrolleghem, P. A. (2007).  
1090 Uncertainty in the environmental modelling process—a framework and guidance.  
1091 *Environmental Modelling & Software*, 22(11), 1543–1556.
- 1092 Ridler, M. E., Zhang, D., Madsen, H., Kidmose, J., Refsgaard, J. C., & Jensen, K. H. (2018).  
1093 Bias-aware data assimilation in integrated hydrological modelling. *Hydrology*  
1094 *Research*, 49(4), 989-1004.
- 1095 Rojas, R., Feyen, L., & Dassargues, A. (2008). Conceptual model uncertainty in groundwater  
1096 modeling: Combining generalized likelihood uncertainty estimation and Bayesian  
1097 model averaging. *Water Resources Research*, 44(12).
- 1098 Rojas, R., Kahunde, S., Peeters, L., Batelaan, O., Feyen, L., & Dassargues, A. (2010).  
1099 Application of a multimodel approach to account for conceptual model and scenario  
1100 uncertainties in groundwater modelling. *Journal of Hydrology*, 394(3), 416–435.
- 1101 Schöniger, A., Wöhling, T., Samaniego, L., & Nowak, W. (2014). Model selection on solid  
1102 ground: Rigorous comparison of nine ways to evaluate Bayesian model evidence.  
1103 *Water resources research*, 50(12), 9484-9513.
- 1104 Schöniger, A., Wöhling, T., & Nowak, W. (2015). A statistical concept to assess the  
1105 uncertainty in Bayesian model weights and its impact on model ranking. *Water*  
1106 *Resources Research*, 51(9), 7524-7546.
- 1107 Singh, A., Mishra, S., & Ruskauff, G. (2010). Model averaging techniques for quantifying  
1108 conceptual model uncertainty. *Groundwater*, 48(5), 701–715.
- 1109 Stedinger, J. R., Vogel, R. M., Lee, S. U., & Batchelder, R. (2008). Appraisal of the  
1110 generalized likelihood uncertainty estimation (GLUE) method. *Water Resources*  
1111 *Research*, 44(12).
- 1112 Trolborg, L., Refsgaard, J. C., Jensen, K. H., & Engesgaard, P. (2007). The importance of  
1113 alternative conceptual models for simulation of concentrations in a multi-aquifer  
1114 system. *Hydrogeology Journal*, 15(5), 843–860.

- 1115 Troldborg, M., Nowak, W., Tuxen, N., Bjerg, P. L., Helmig, R., & Binning, P. J. (2010).  
1116 Uncertainty evaluation of mass discharge estimates from a contaminated site using a  
1117 fully Bayesian framework. *Water Resources Research*, 46(12).
- 1118 Tsai, F. T. C. (2010). Bayesian model averaging assessment on groundwater management  
1119 under model structure uncertainty. *Stochastic Environmental Research and Risk  
1120 Assessment*, 24(6), 845-861.
- 1121 Tsai, F. T. C., & Elshall, A. S. (2013). Hierarchical Bayesian model averaging for  
1122 hydrostratigraphic modeling: Uncertainty segregation and comparative evaluation.  
1123 *Water Resources Research*, 49(9), 5520-5536.
- 1124 Van Straten, G. T., & Keesman, K. J. (1991). Uncertainty propagation and speculation in  
1125 projective forecasts of environmental change: A lake-eutrophication example. *Journal  
1126 of Forecasting*, 10(1-2), 163–190.
- 1127 Vrugt, J. A. (2016). Markov chain Monte Carlo simulation using the DREAM software  
1128 package: Theory, concepts, and MATLAB implementation. *Environmental Modelling  
1129 & Software*, 75, 273-316.
- 1130 Vrugt, J. A. (2016a). *MODELAVG: A MATLAB Toolbox for Postprocessing of Model  
1131 Ensembles* (Vol. Manual). Department of Civil and Environmental Engineering,  
1132 University of California Irvine, 4130 Engineering Gateway, Irvine, CA.
- 1133 Vrugt, J. A., & Robinson, B. A. (2007). Treatment of uncertainty using ensemble methods:  
1134 Comparison of sequential data assimilation and Bayesian model averaging. *Water  
1135 Resources Research*, 43(1).
- 1136 Vrugt, J. A., Ter Braak, C. J., Clark, M. P., Hyman, J. M., & Robinson, B. A. (2008).  
1137 Treatment of input uncertainty in hydrologic modeling: Doing hydrology backward  
1138 with Markov chain Monte Carlo simulation. *Water Resources Research*, 44(12).
- 1139 Vrugt, J. A., Ter Braak, C. J. F., Diks, C. G. H., Robinson, B. A., Hyman, J. M., & Higdon,  
1140 D. (2009a). Accelerating Markov chain Monte Carlo simulation by differential  
1141 evolution with self-adaptive randomized subspace sampling. *International Journal of  
1142 Nonlinear Sciences and Numerical Simulation*, 10(3), 273-290.
- 1143 Vrugt, J. A., Ter Braak, C. J., Gupta, H. V., & Robinson, B. A. (2009b). Equifinality of  
1144 formal (DREAM) and informal (GLUE) Bayesian approaches in hydrologic  
1145 modeling?. *Stochastic environmental research and risk assessment*, 23(7), 1011-1026.
- 1146 Vrugt, J. A., ter Braak, C. J., Diks, C. G., & Schoups, G. (2013). Hydrologic data assimilation  
1147 using particle Markov chain Monte Carlo simulation: Theory, concepts and  
1148 applications. *Advances in Water Resources*, 51, 457-478.

1149 Wasserman, L. (2000). Bayesian model selection and model averaging. *Journal of*  
1150 *mathematical psychology*, 44(1), 92-107.

1151 Xue, L., & Zhang, D. (2014). A multimodel data assimilation framework via the ensemble  
1152 Kalman filter. *Water Resources Research*, 50(5), 4197-4219.

1153 Yang, J., Reichert, P., Abbaspour, K. C., Xia, J., & Yang, H. (2008). Comparing uncertainty  
1154 analysis techniques for a SWAT application to the Chaohe Basin in China. *Journal of*  
1155 *Hydrology*, 358(1), 1–23.

1156 Ye, M., Neuman, S. P., & Meyer, P. D. (2004). Maximum likelihood Bayesian averaging of  
1157 spatial variability models in unsaturated fractured tuff. *Water Resources Research*,  
1158 40(5).

1159 Ye, M., Pohlmann, K. F., Chapman, J. B., Pohll, G. M., & Reeves, D. M. (2010). A model-  
1160 averaging method for assessing groundwater conceptual model uncertainty.  
1161 *Groundwater*, 48(5), 716–728.

1162 Yin, J., & Tsai, F. T. C. (2018). Saltwater scavenging optimization under surrogate  
1163 uncertainty for a multi-aquifer system. *Journal of hydrology*, 565, 698-710.

1164 Zhou, Y., & Herath, H. M. P. S. D. (2017). Evaluation of alternative conceptual models for  
1165 groundwater modelling. *Geoscience Frontiers*, 8(3), 437-443.

1166

1167

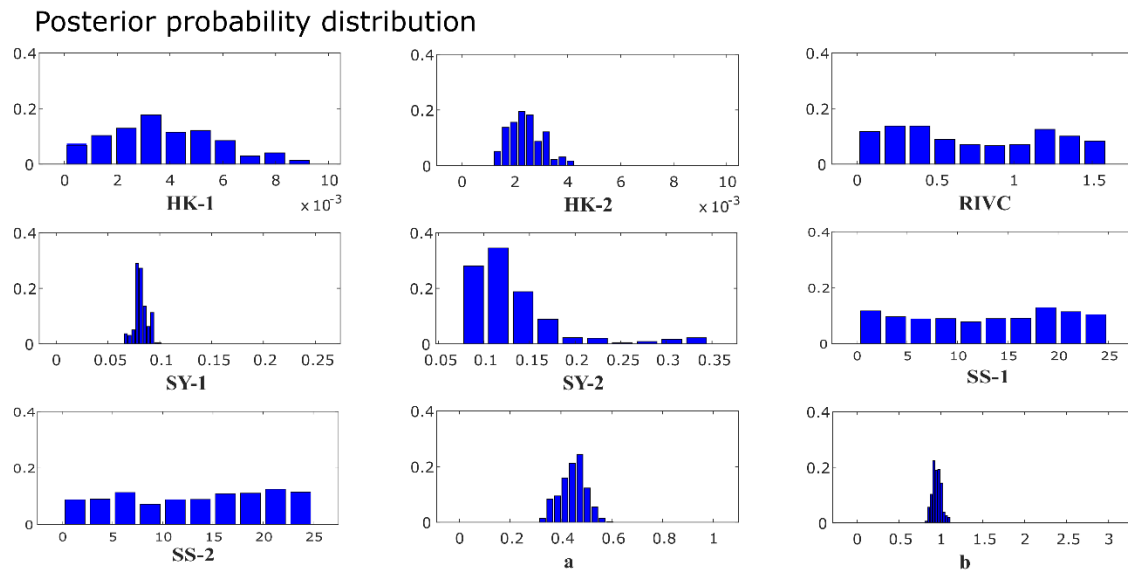
1168

1169

1170

1171

1172 **Supplementary material**



1173  
 1174 **Supplementary Figure 2.** The posterior probability distribution of the L2B4 model  
 1175 parameters and the parameters of the heteroscedastic error-model (A and B) for scenario 1,  
 1176 using 2500 samples generated after convergence.

1177

1178 **Supplementary Table 3.** Percentage observation coverage of the parameter uncertainty band  
 1179 and calculated d-factor based on the total uncertainty band for all the conceptual models.

	L1B5		L2B4		L2B5		L3B5	
	% cover	d-factor	% cover	d-factor	% cover	d-factor	% cover	d-factor
Scenario 1	8.5	1.88	12.0	2.03	13.8	2.01	13.0	2.04
Scenario 2	31.0	1.59	26.8	1.94	24.8	1.89	26.16	1.88

1180 **Supplementary Table 2.** Correlations between the groundwater level predictions using  
 1181 different conceptual models.

	L1B5	L2B4	L2B5	L3B5
L1B5	1	-0.495	-0.367	-0.491
L2B4		1	-0.125	-0.119
L2B5			1	-0.072
L3B5				1

1182